

2 **Synthesis, Spectral and Thermal Characterization of**
3 **Selected Metal Complexes Containing Schiff Base**
4 **Ligands with Antimicrobial Activities**
5
6
7

8 Abstract

9 Selected metal complexes of Ni(II), Zn(II), Mn(II), Sn(II), Co(II) and Cd(II) ions were
10 synthesized with three different synthesized Schiff base ligands. The ligands and metal
11 complexes were isolated in solid state from the reaction medium and characterized by molar
12 conductivity measurement, magnetic susceptibility, Infrared, electronic spectral, thermal
13 analysis and some physical measurements. The overall reactions were monitored by TLC
14 analysis. Molar conductance study have shown that all the complexes were non electrolytic in
15 nature. FTIR studies suggested that Schiff bases act as deprotonated bidentate ligands and
16 metal ions are attached with the ligands through N, O/S coordinating sites during
17 complexation reaction. Magnetic susceptibility data coupled with electronic spectra revealed
18 that Zn(II), Mn(II), Sn(II), and Cd(II) complexes have tetrahedral, Ni(II) complexes has square
19 planer and Co(II) complexes has octahedral geometry. Thermal analysis (TGA and DTG) data
20 showed the possible degradation pathway of the complexes and also indicated that most of
21 the complexes were thermally stable up to 200⁰C. The Schiff bases and their metal complexes
22 have been found moderate to strong antimicrobial activity.

23 Keywords: Schiff Base, Thiosemicarbazide, TGA, DTG, Antimicrobial activity

24 **1. INTRODUCTION**

25 Multidentate ligands are extensively used for the preparation of metal complexes with
26 interesting properties [1-5]. Among these ligands, Schiff bases containing nitrogen and
27 phenolic oxygen donor atoms are of considerable interest due to their potential application in
28 catalysis, medicine and material science [6-9]. Transition metal complexes of these ligands
29 exhibit varying configurations, structural liability and sensitivity to molecular environments.
30 The central metal ions in these complexes act as active sites for pharmacological agent.
31 This feature is employed for modeling active sites in biological systems.

32 Thiosemicarbazones obtained by the condensation reaction of thiosemicarbazide and
33 different aldehydes or ketones are important chemicals due to their broad profile of
34 pharmacological activity. The transition metal complexes of thiosemicarbazone are also
35 played important role in antimicrobial, antitumor and anticancer activities.

36 Therefore, in view of our interest in synthesis of new Schiff base complexes, which might
37 find application as pharmacological and as luminescence probes, we have synthesized and
38 characterized new transition metal complexes of Schiff bases formed by the condensation
39 reaction of different aldehydes and amino acids. The results of our studies are presented in
40 this article.

41 **2. Experimental**

42 **2.1 Materials and Methods**

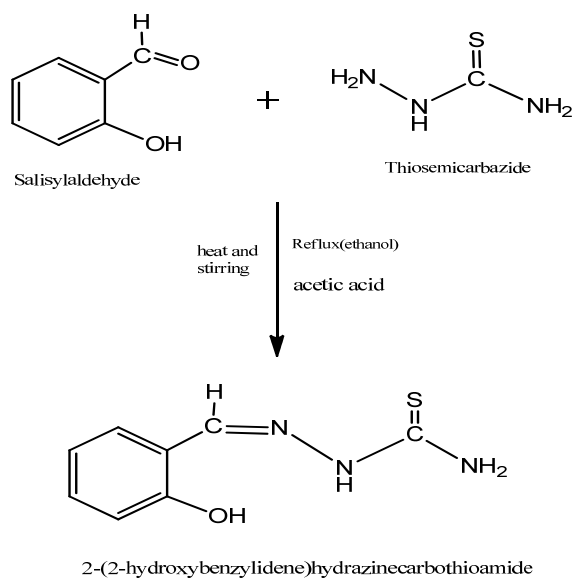
43 All chemicals and solvents used were of Analar grade. All metal(II) salts were used as
44 chloride and sulphate. The solvents such as Ethanol, methanol, chloroform, Diethyl ether,
45 petroleum ether, DMSO (dimethyl sulfoxide) and acetonitrile were purified by standard
46 procedure. The melting point or the decomposition temperature of all the prepared ligand and
47 metal complexes were observed in an electro thermal melting point apparatus model No.
48 AZ6512. Vibrational spectra (IR) were recorded with a NICOLET 310, FTIR
49 spectrophotometer, Belgium, in the range $4000-225\text{ cm}^{-1}$ with a KBr disc as reference. UV-
50 Visible spectra of the complexes in DMSO ($0.5 \times 10^{-3}\text{ M}$) were recorded in the region 200-800
51 nm on a Thermoelectron Nicolet evolution 300 UV-Visible spectrophotometer. The
52 SHERWOOD SCIENTIFIC Magnetic Susceptibility Balance that following the Gouy
53 Method were used to measure the magnetic moment of the solid complexes. The electrical
54 conductance measurements were made at room temperature in freshly prepared aqueous
55 solution (10^{-3} M) and in DMSO using a WPACM35 conductivity meter and a dip-cell with a
56 platinum electrode. The thermogravimetric analyses (TGA) were performed on Perkin Elmer
57 Simultaneous Thermal Analyzer, STA-8000. The purity of the ligand and metal complexes
58 were tested by Thin Layer Chromatography (TLC).

59

60 **2.1 Synthesis of Schiff base Ligand $\text{C}_8\text{H}_9\text{ON}_3\text{S}$ (L^1)**

61 The ligand was prepared by condensation reaction of 20 mmole of salicylaldehyde (1.048ml)
62 with 20 mmole (1.82gm) of thiosemicarbazide in a clean round bottomed flask.
63 Salicylaldehyde was dissolved in 20ml ethanol and thiosemicarbazide was dissolved in hot

64 ethanol with water. The solutions were mixed and refluxed for 3-4 hours. On cooling off
65 white colored product was formed which was washed with ethanol, acetone, and diethyl ether
66 and dried in vacuum desiccators over anhydrous CaCl_2 . The purity of ligand was tested by
67 TLC using different solvents. The product was found to be soluble in methanol, chloroform
68 and DMSO. It provided 80% yield at 34°C . The target Schiff base was synthesized according
69 to Schema-1.

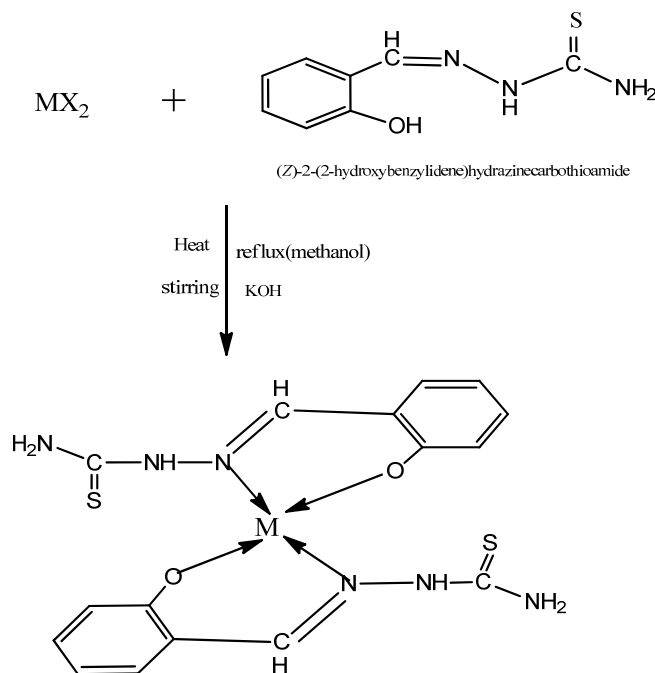


70

71 Schema 1: Synthetic pathway of Schiff base ligand $\text{C}_{14}\text{H}_{11}\text{O}_3\text{N}$ (L^1)

72 2.3 Synthesis of Metal Complexes Using Schiff Base Ligand $\text{C}_{14}\text{H}_{11}\text{O}_3\text{N}$ (L^1)

73 The synthesized complexes have the general formula $[\text{M}(\text{SB})_2]$; where $\text{M} = \text{Zn}(\text{II}), \text{Ni}(\text{II})$ and
74 $\text{Mn}(\text{II})$ and $\text{SB} =$ synthesized Schiff base ligand (Schema 2). During complexation
75 reaction, 15ml methanolic solution of Zinc(II) sulphate (0.2875g, 1mmol)/ Ni(II) chloride
76 hexahydrate (0.238g, 1mmol)/ Manganese(II) chloride tetrahydrate (0.198g, 1mmol) was
77 taken in a two necked round bottom flask and kept on a magnetic stirring. A methanolic
78 solution (20 mL) of prepared Schiff base ligand (0.390g, 2mmol) was added drop wise and a
79 methanolic solution (10mL) of KOH (0.1122g, 1mmol) was added slowly then the resultant
80 mixture was heated with constant stirring on a magnetic stirrer for 4-5 hours. On cooling
81 colored solid product was formed which was washed with methanol, acetone, ether and dried
82 in vacuum over anhydrous CaCl_2 . The reaction was monitored by TLC using petroleum ether,
83 toluene, ethyl acetate and methanol as solvent. The common structure of metal complexes has
84 been shown in Schema-1 and individual expected structures of the complexes are shown as
85 supplementary materials.



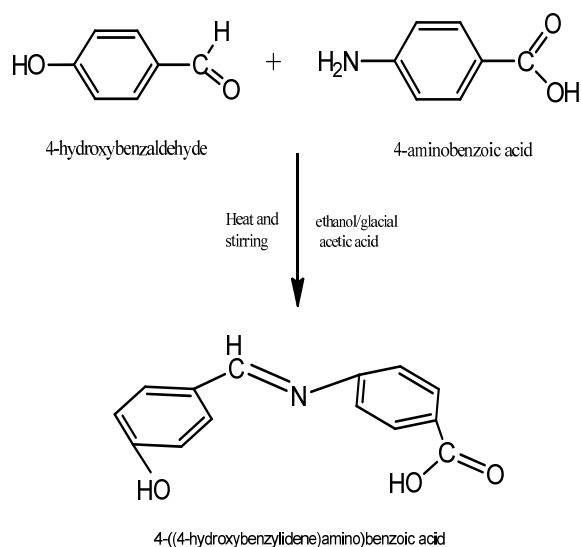
86

87 Schema 2: Synthetic pathway of Schiff Base Ligand (L^2) Metal Complexes, with $M=\text{Zn(II)}$,
 88 Ni(II) , Mn(II) , and Sn(II) ions and $X=\text{Cl}^-$, SO_4^{2-} ions

89

90 2.4 Synthesis of Schiff Base Ligand $\text{C}_{14}\text{H}_{11}\text{O}_3\text{N}$ (L^2)

91 4-hydroxy benzaldehyde (2.44g, 20 mmol) dissolved in absolute ethanol (20-25 mL) was
 92 added dropwise to a constant stirring solution of 4-aminobenzoic acid(2.76 g, 20 mmol) in 30
 93 mL ethanol and 2 mL of conc. glacial acetic acid was added slowly. Then the mixture was
 94 refluxed for (4-5)h. On cooling, a solid yellow product was formed which was filtered,
 95 washed with ethanol and diethyl ether and dried in vacuum over anhydrous CaCl_2 . The
 96 reaction was monitored by TLC using petroleum ether, ethyl acetate, toluene and methanol
 97 solvents. The product was found to be soluble in methanol, chloroform and DMSO. It
 98 provided 65% yield at 34°C . The target Schiff base was synthesized according to Schema-3.

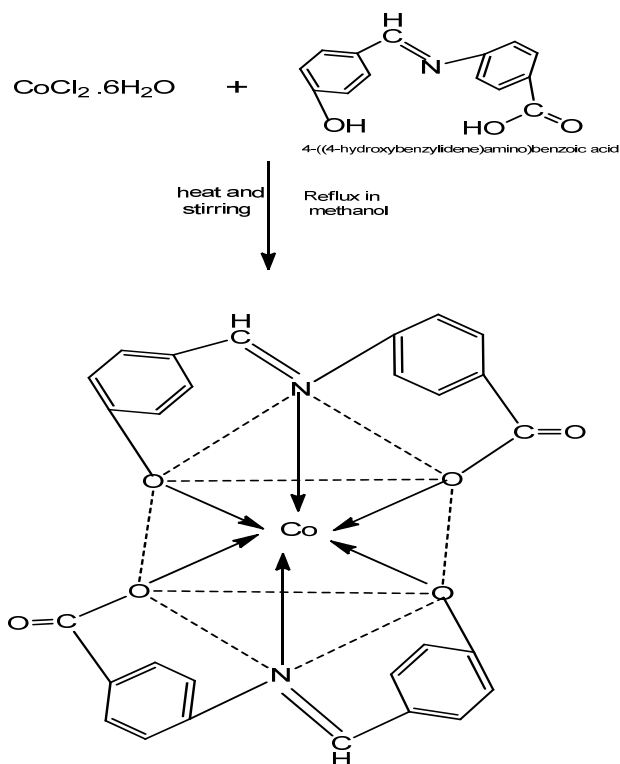


99

100 Schema-3: Synthetic pathway of Schiff base ligand $C_{14}H_{11}O_3N$ (L^2)

101 **2.5 Synthesis of Metal Complex Using Schiff Base Ligand (L^2)**

102 The complex was prepared in 1:2 molar ratio (metal : ligand). A methanolic solution (20
 103 mL) of cobalt(II) chloride hexahydrate (0.24 g, 1 mmol)) was taken in a two necked round
 104 bottom flask and kept on magnetic stirring and a methanolic solution (20 mL) of prepared
 105 Schiff base ligand (0.483 g, 2 mol) was added dropwise and stirred with heating for 4-5h. On
 106 cooling, precipitate was formed which was filtered, washed with ethanol, acetone, and diethyl
 107 ether and dried in vacuum desiccators over anhydrous $CaCl_2$. The purity of complex was
 108 tested by TLC using different solvents. The complex was soluble in DMSO with heat. The
 109 proposed structure of complex is shown in Schema-4.

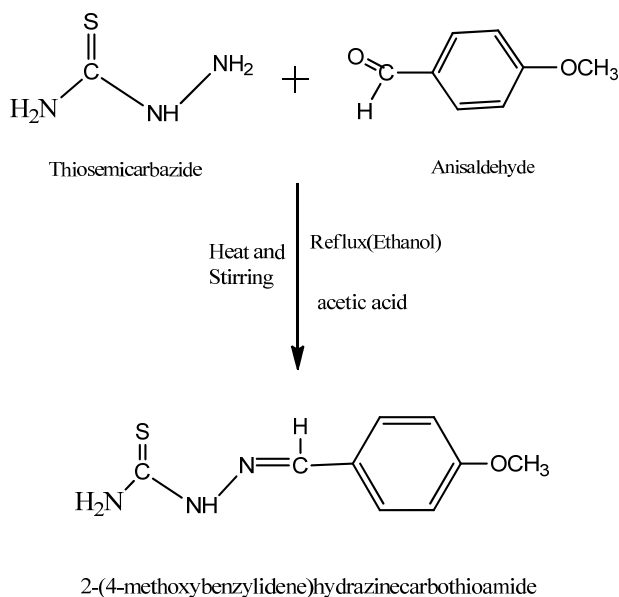


110

111 Schema-4: Synthetic pathway of Co(II) complex with Schiff Base Ligand (L^2)

112 **2.6 Synthesis of Schiff base Ligand $C_9H_{11}N_3OS$ (L^3)**

113 To a stirring solution of thiosemicarbazide (0.91 gm, 10 mmol) dissolved in 20mL of ethanol
 114 with water, a solution of Anisaldehyde(1.22mL,10mmol) in 10mL ethanol was added dropwise.
 115 After sometime 2ml of glacial acetic acid was added with the reaction mixture and the solution
 116 was refluxed for 5-6 h and allowed to cool overnight in room temperature. The off white
 117 product was filtered washed several times with ethanol and finally with diethyl ether and dried in
 118 vacuum over anhydrous CaCl_2 . The reaction was monitored by TLC using petroleum ether,
 119 ethyl acetate, toluene and methanol solvents .The product was found to be soluble in methanol,
 120 DMF and DMSO. It provided 62% yield. The Schiff base was synthesized according to
 121 Schema-5.



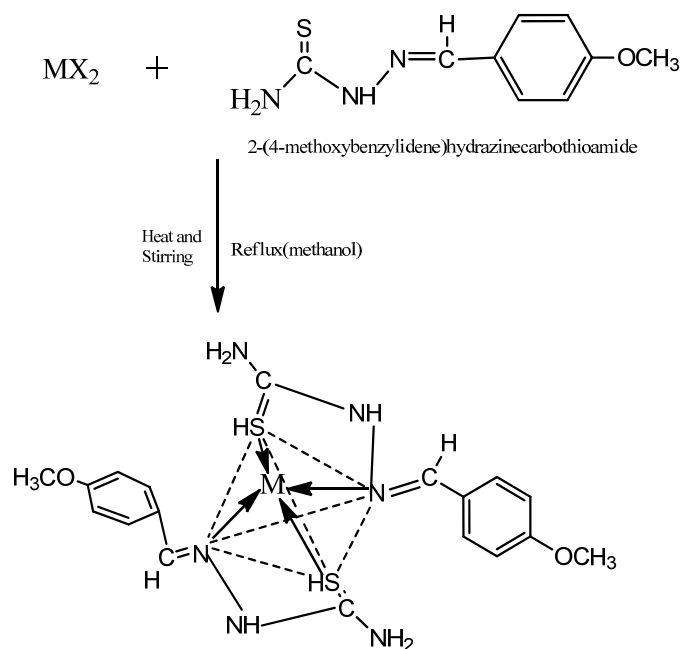
122

123

Schema-5: Synthetic pathway of Schiff base ligand $C_9H_{11}N_3OS$ (L^3)

124 **2.7 Synthesis of Metal Complex Using Schiff Base Ligand (L^3):**

125 The complex was prepared in 1:2 molar ratio (metal : ligand). Methanolic solution (20 mL) of
 126 cadmium(II) chloride dihydrate (0.228g, 1mmol) was taken in a two necked round bottom
 127 flask and kept on magnetic stirring. A methanolic solution (20 mL) of prepared Schiff base
 128 ligand (L^3) (0.418g, 2mmol) was added dropwise and stirred with heating for 4-5h. On
 129 cooling, precipitate was formed which was filtered, washed with ethanol, acetone, and diethyl
 130 ether and dried in vacuum desiccators over anhydrous $CaCl_2$. The reaction was monitored by
 131 TLC using different solvents. The complex was soluble in DMSO with heat. The proposed
 132 structure of complex is shown in Schema-6.



133

134 Schema-6: Synthetic pathway of Schiff Base Ligand (L^4) Metal Complex

135

Where, $M=\text{Cd}(\text{II})$ ions

136 3. Characterization of the Ligands and Complexes

137 The structures of the complexes were characterized by melting point, conductivity
 138 measurements, magnetic susceptibility, IR spectra and UV visible spectra [10] analysis. The
 139 purity of the ligands and metal complexes were monitored by Thin Layer Chromatography
 140 (TLC). The ligands and complexes are characterized below by these methods.

141

142 3.1 Melting point

143 Melting point gives an approximate idea about the nature of the complexes and can suggest
 144 whether it is covalent or ionic [11]. The melting point of all the synthesized ligands and
 145 complexes are shown in Table-1.

146

147 **Table-1:** Physical characteristics and analytical data of ligands and complexes

Compound/Empirical Formula	Formula Weight	Color	Yield(%)	Melting Point/ Decomposition temp.($^{\circ}\text{C}$)
Ligand (L^1) $\text{C}_8\text{H}_9\text{ON}_3\text{S}$	195	off white	80 %	$215^{\circ}\text{C} - 217^{\circ}\text{C}$

[Zn (L ¹) ₂].2H ₂ O [ZnC ₁₆ H ₁₆ O ₂ N ₆ S ₂].2H ₂ O	491.38	cream color	67 %	above 300 ⁰ C
[Ni (L ¹) ₂].H ₂ O [NiC ₁₆ H ₁₆ O ₂ N ₆ S ₂].H ₂ O	466.93	yellow green	70 %	275 ⁰ C - 280 ⁰ C
[Mn (L ¹) ₂].H ₂ O [MnC ₁₆ H ₁₆ O ₂ N ₆ S ₂].H ₂ O	462.94	golden rod	65 %	275 ⁰ C - 280 ⁰ C
[Sn (L ¹) ₂] [SnC ₁₆ H ₁₆ O ₂ N ₆ S ₂]	508.71	greenish yellow	60%	240 ⁰ C - 250 ⁰ C
Ligand (L ²) C ₁₄ H ₁₁ O ₃ N	241	yellow	65 %	241 ⁰ C - 245 ⁰ C
[Co(L ²) ₂].2H ₂ O [CoC ₂₈ H ₁₈ O ₆ N ₂].2H ₂ O	576.93	golden rod	56 %	above 300 ⁰ C
Ligand (L ³) C ₉ H ₁₁ N ₃ OS	209	off white	62%	145 ⁰ C - 150 ⁰ C
[Cd(L ³) ₂] [CdC ₁₈ H ₂₂ O ₂ N ₆ S ₂]	530.41	white	75 %	260 ⁰ C - 265 ⁰ C

148

149 3.2 Conductivity

150

151 The molar conductivities were obtained using the formula

$$152 \quad \Lambda = \frac{1000}{C} \times \text{Cell constant} \times \text{Observed conductivity}, \quad (1).$$

153 where, Λ =molar conductance, C = concentration.

154 The molar conductance is calculated from the measured specific conductance at room
155 temperature by using the above equation. The experimental results are shown in Table-2.

156

157 **Table-2:** Data for the determination of Molar conductivity

Name of Complex	Observed conductivity (ohm ⁻¹ cm ² mol ⁻¹)	Molar conductance Λ $= (1000/c)$ $\times \text{specific conductance}$ $\text{Scm}^2 \text{mol}^{-1}$	μ_{eff} in B.M.	No. of unpaired electron
[Zn (L ¹) ₂].2H ₂ O [ZnC ₁₆ H ₁₆ O ₂ N ₆ S ₂].2H ₂ O	3	3	0.567	–
[Ni (L ¹) ₂].H ₂ O [NiC ₁₆ H ₁₆ O ₂ N ₆ S ₂].H ₂ O	6	6	1.471	–
[Mn (L ¹) ₂].H ₂ O [MnC ₁₆ H ₁₆ O ₂ N ₆ S ₂].H ₂ O	8	8	2.576	1
[Sn (L ¹) ₂] [SnC ₁₆ H ₁₆ O ₂ N ₆ S ₂]	9	9	0.639	–
[Co(L ²) ₂].2H ₂ O [CoC ₂₈ H ₁₈ O ₆ N ₂].2H ₂ O	8	8	4.017	3
[Cd(L ³) ₂] [CdC ₁₈ H ₂₂ O ₂ N ₆ S ₂]	6	6	0.461	–

158

159 From the above table data it is showed that all the complexes are non-electrolyte.

160 3.3 Characterizations by Magnetic Susceptibility

161 **Measurement of magnetic susceptibility:** The measurements of magnetic susceptibilities
162 were made at about constant temperature; Curie-law was used and was calculated from the
163 equation.

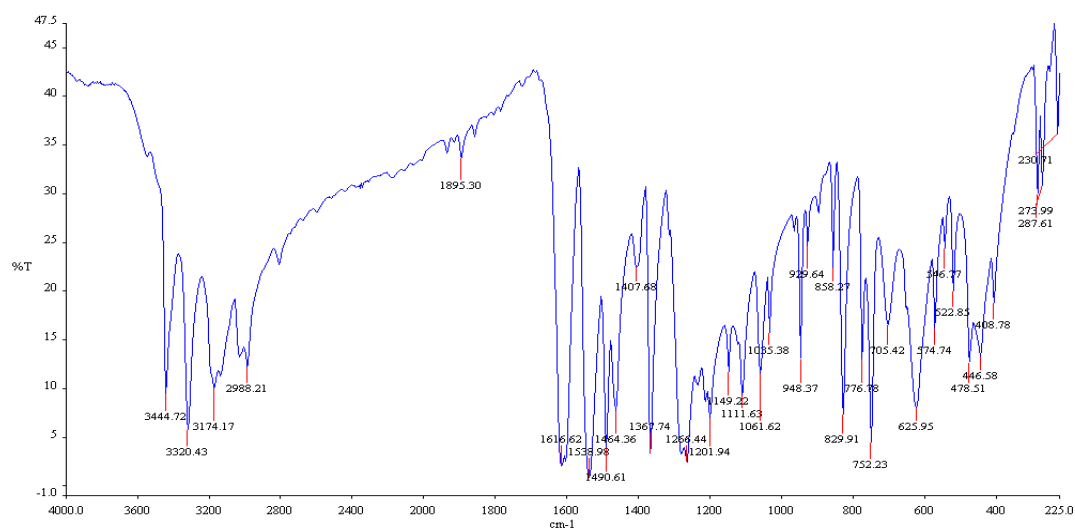
$$164 \quad \mu_{\text{eff}} = 2.83 \sqrt{\chi_m^{\text{corr}} \cdot T} \quad \text{B.M.} \quad (2)$$

165 Thus μ_{eff} obtained is known as effective magnetic moment. All the values and weight were
166 expressed in C.G.S. units. The observed values of effective magnetic moment (μ_{eff}) of the
167 complexes at room temperature are given in table 2. From the above data it is showed that the
168 Zn(II), Ni(II), Sn(II) and Cd(II) ions complexes are diamagnetic and Mn(II) and Co(II) ions
169 complexes are paramagnetic in nature[13].

170 **3.4 Measurement of IR spectra:** At first the complexes heat six hour and KBr overnight in oven.
171 Then the complexes and KBr grind with pestle in mortar. Infrared spectra disc were recorded as
172 KBr with a NICOLET 310, FTIR spectrophotometer, Belgium, from 4000-225 cm⁻¹.

173 **3.4.1 IR spectra of Schiff Base ligand C₈H₉ON₃S (L¹) and It's metal complexes**

174 The spectrum of ligand showed a strong absorption band at 1616 cm⁻¹ due to the azomethine
175 $\nu(\text{C}=\text{N})$ stretching frequency of the free ligand [14-18] indicating that the condensation have
176 taken place between the CHO moiety of salicylaldehyde and -NH₂ moiety of
177 thiosemicarbazide. The IR spectra of the free ligand (figure-1) showed two bands at 3320 cm⁻¹
178 ¹ and 3174 cm⁻¹ may be attributed to the free -NH₂ and $\nu(\text{N}-\text{H})$ groups respectively. These
179 bands remains in the same region in all complexes spectra, suggesting nonparticipation in
180 coordination of one terminal -NH₂ group in thiosemicarbazone [15,19-21] The band
181 observed at 3444 cm⁻¹ was assigned to the $\nu(\text{O}-\text{H})$ of hydroxyl group [14,15,22]. The strong
182 band 776 cm⁻¹ for $\nu(\text{C}=\text{S})$ indicated that C=S bond was present in the Schiff base ligand
183 [14,22].



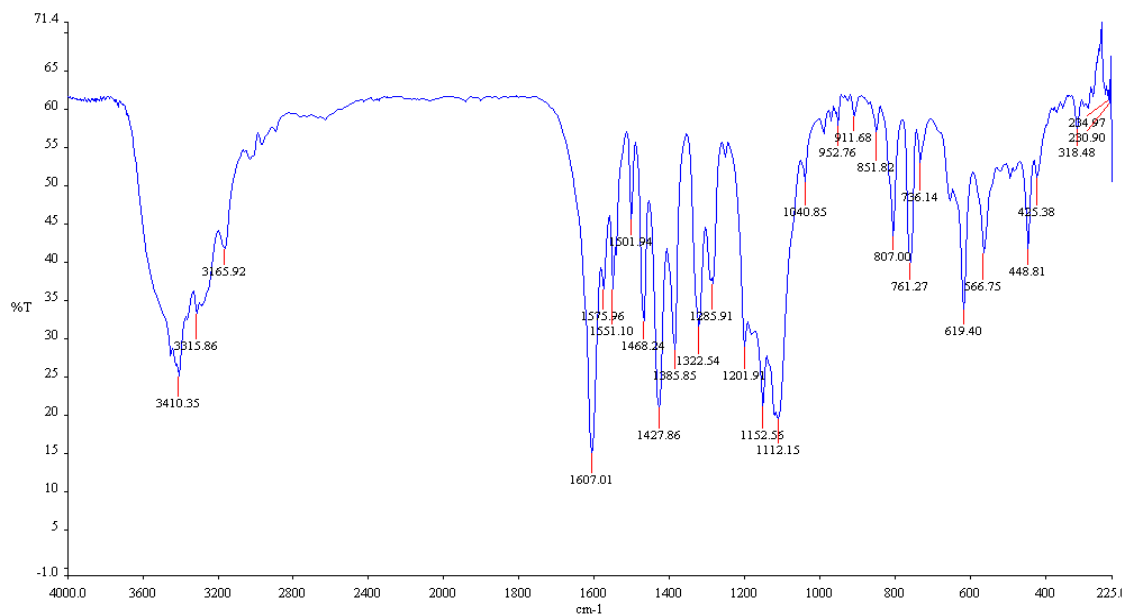
184

185 Figure-1: IR spectra of Schiff base ligand C₈H₉ON₃S (L¹)

186

187 In order to determine the mode of coordination of ligand to metal in complexes, IR spectrum
188 of ligand was compared with IR spectrum of metal complexes (figure-2). The band at 1616
189 cm⁻¹ due to the azomethine $\nu(\text{C}=\text{N})$ stretching frequency of the free ligand that shifted to
190 lower frequency in the spectra of the Zn (II) complex at 1607 cm⁻¹ which indicated the
191 coordination through azomethine N atom. The band 3444 cm⁻¹ due to the $\nu(\text{O}-\text{H})$ of hydroxyl
192 group in the IR spectra of the ligand was absent and shifted to lower absorption frequency in
193 the IR spectra of Ni(II) complex indicated the coordination through the phenolic oxygen
194 [23,24]. This is confirmed by the shift of $\nu(\text{C}-\text{O})$ stretching vibration observed at 1266cm⁻¹
195 in the spectra of free ligand to 1285 cm⁻¹ stretching vibration of complex after coordination

196 [16], which corresponds to forming of weaker C-O(Zn) bond comparing to C-O(H) and
 197 confirms coordination of ligand to Ni(II) via deprotonated phenolic oxygen [25,26]. Also the
 198 medium intensity bands observed at 566 cm⁻¹ is attributed to M-O and 448 cm⁻¹ is attributed
 199 to M-N bonds [27]. IR spectral components of the synthesized complexes are shown in Table
 200 – 3.



201

Figure-2: IR spectra of [ZnC₁₆H₁₆O₂N₆S₂].2H₂O complex

202

203 **Table-3:** FTIR spectral data of the ligand C₈H₉ON₃S (L¹) and it's metal complexes (in cm⁻¹)

Ligand / Metal Complexes	IR/cm ⁻¹				
	ν(O-H)	ν(C=N)	ν(C-O)	ν(M-O)	ν(M-N)
C ₈ H ₉ ON ₃ S	3444	1616	1266	-	-
[ZnC ₁₆ H ₁₆ O ₂ N ₆ S ₂].2H ₂ O	3410	1607	1285	566	448
[NiC ₁₆ H ₁₆ O ₂ N ₆ S ₂].H ₂ O	3412	1607	1294	567	457
[MnC ₁₆ H ₁₆ O ₂ N ₆ S ₂].H ₂ O	3413	1600	1296	570	442
[SnC ₁₆ H ₁₆ O ₂ N ₆ S ₂]	3436	1610	1286	594	458

204

205 **3.4.2 IR spectra of Schiff Base ligand C₁₄H₁₁O₃N (L²) and It's metal complex**

206 The bands at 1735 cm^{-1} and 3420 cm^{-1} due to carbonyl (C=O) and NH_2 stretching vibrations
207 of the starting reagents respectively were absent in the spectra of ligand and a strong new
208 band at 1620 cm^{-1} was appeared which assigned to the azomethine (HC=N) linkage, a
209 fundamental feature of Schiff base ligand [28,29]. This indicated that amino and aldehyde
210 moieties of the starting reagents have been converted into the azomethine moiety. The bands
211 at 1320 cm^{-1} due to $\nu(\text{C-O})$ of phenolic group and 3410 cm^{-1} due to the phenolic $\nu(\text{OH})$ were
212 also observed in the spectra of ligand [23]. The bands at 1680 cm^{-1} due to $\nu(\text{C=O})$ stretching
213 vibration and 3080 cm^{-1} due to carboxylic $-\nu(\text{OH})$ were observed in the IR spectra of ligand
214 [30-33].

215

216 The band at 1620 cm^{-1} due to the azomethine $-\text{HC=N}$ stretching vibration was shifted to
217 lower frequency at 1541 cm^{-1} in the metal complex compared to free ligand, suggested the
218 coordination of metal ion through nitrogen of azomethine group [34-36]. The N atom of
219 azomethine would reduce the electron density in the azomethine link and thus lower the $-\text{HC=N}$
220 absorption after coordination. This is further substantiate by the presence of a new
221 band at 457 cm^{-1} assignable to $\nu(\text{M-N})$. The disappearance of phenolic $\nu(\text{OH})$ band at 3410 cm^{-1}
222 in Co(II) complex suggested the co-ordination by the phenolic oxygen after
223 deprotonation to the metal ions. This is further supported by shifting of $\nu(\text{C-O})$ phenolic
224 band at 1320 cm^{-1} to lower wave number at 1305 cm^{-1} in the metal complex. The appearance
225 of a new band at 590 cm^{-1} due to $\nu(\text{M-O})$ in the Co(II) complex which further substantiate .
226 The band at 1680 cm^{-1} assigned to $\nu(\text{C=O})$ in the spectra of ligand also shifted to lower
227 frequency range in the metal complex. That suggested the involvement of oxygen atom of
228 carboxylic $\nu(-\text{OH})$ group to the coordination with metal ions. The comparison of the IR
229 spectra of the Schiff base and it's metal chelates indicated that the Schiff base ligand
230 coordinated to metal ions by three donor atoms representing the ligand acting in a tri-
231 dentative manner. Spectral data of $[\text{CoC}_{28}\text{H}_{18}\text{O}_6\text{N}_2]\cdot 2\text{H}_2\text{O}$ is shown in Table 4.

232 In order to determine the mode of coordination of ligand to metal in complexes IR spectrum
233 of ligand was compared with IR spectrum of metal complexes [14, 23]. The band at 1616 cm^{-1}
234 due to the azomethine $\nu(\text{C=N})$ stretching frequency of the free ligand that shifted to lower
235 frequency in the spectra of the Ni(II) complex (figue-13) at 1607 cm^{-1} indicating the
236 coordination through N atom [5-9]. The band 3444 cm^{-1} due to the $\nu(\text{O-H})$ of hydroxyl
237 group in the IR spectra of the ligand was absent and shifted to lower absorption frequency in

238 the IR spectra of Ni(II) complex indicated the coordination through the phenolic oxygen
239 [22,24]. This is confirmed by the shift of $\nu(\text{C-O})$ stretching vibration observed at 1266 cm^{-1}
240 in the spectra of free ligand to 1294 cm^{-1} stretching vibration of complex after coordination
241 [16], which corresponds to forming of weaker C-O(Ni) bond comparing to C-O(H) and
242 confirms coordination of ligand to Ni(II) via deprotonated phenolic oxygen. Also the medium
243 intensity bands observed at 567 cm^{-1} is attributed to M-O and 457 cm^{-1} is attributed to M-N
244 bonds [27].

245 The band at 1616 cm^{-1} due to the azomethine $\nu(\text{C=N})$ stretching frequency of the free ligand
246 that shifted to lower frequency in the spectra of the Mn(II) complex at 1600 cm^{-1} indicating
247 the coordination through N atom. The band 3444 cm^{-1} due to the $\nu(\text{O-H})$ of hydroxyl group
248 in the IR spectra of the ligand was absent and shifted to lower absorption frequency in the IR
249 spectra of Mn(II) complex indicated the coordination through the phenolic oxygen. This is
250 confirmed by the shift of $\nu(\text{C-O})$ stretching vibration observed at 1266 cm^{-1} in the spectra of
251 free ligand to 1296 cm^{-1} stretching vibration of complex after coordination, which
252 corresponds to forming of weaker C-O(Mn) bond comparing to C-O(H) and confirms
253 coordination of ligand to Mn(II) via deprotonated phenolic oxygen [5,17]. Also the medium
254 intensity bands observed at 570 cm^{-1} is attributed to M-O and 442 cm^{-1} is attributed to M-N
255 bonds [27].

256 The band at 1616 cm^{-1} due to the azomethine $\nu(\text{C=N})$ stretching frequency of the free ligand
257 that shifted to lower frequency in the spectra of the Sn(II) complex at 1610 cm^{-1} indicating
258 the coordination through N atom. The band 3444 cm^{-1} due to the $\nu(\text{O-H})$ of hydroxyl group in
259 the IR spectra of the ligand was absent and shifted to lower absorption frequency in the IR
260 spectra of Sn(II) complex indicated the coordination through the phenolic oxygen. This is
261 confirmed by the shift of $\nu(\text{C-O})$ stretching vibration observed at 1266 cm^{-1} in the spectra of
262 free ligand to 1286 cm^{-1} stretching vibration of complex after coordination, which
263 corresponds to forming of weaker C-O(Sn) bond comparing to C-O(H) and confirms
264 coordination of ligand to Sn(II) via deprotonated phenolic oxygen. Also the medium
265 intensity bands observed at 594 cm^{-1} is attributed to M-O and 458 cm^{-1} is attributed to M-N
266 bonds.

267

268 **Table-4:** FTIR spectral data of the ligand L^2 and $[\text{CoC}_{28}\text{H}_{18}\text{O}_6\text{N}_2]\cdot 2\text{H}_2\text{O}$ (in cm^{-1})

Ligand / Metal Complexes	IR/cm ⁻¹					
	$\nu(\text{O-H})$	$\nu(\text{C=N})$	$\nu(\text{C=O})$	$\nu(\text{C-O})$	$\nu(\text{M-O})$	$\nu(\text{M-N})$
C ₁₄ H ₁₁ O ₃ N	3410	1620	1680	1320	-	-
[CoC ₂₈ H ₁₈ O ₆ N ₂].2H ₂ O	3436	1541	1598	1305	590	457

269

270 3.4.3 IR spectra of Schiff Base ligand C₉H₁₁N₃OS (L³) and It's metal complex

271 The peaks obtained at 3406cm⁻¹ and 3291cm⁻¹ may be assigned to symmetric and asymmetric
 272 $\nu(-\text{N-H})$ stretching frequency of primary amino group. The broad peak obtained between
 273 3282 and 2829 cm⁻¹ may be assigned to overlapping of peaks of hydrogen bonded $\nu(\text{N-H})$
 274 and aromatic C-H stretching frequency. The bands obtained between 1183 cm⁻¹ and 1252 cm⁻¹
 275 ¹ in ligand were due to $\nu(-\text{OCH}_3)$ groups (Table-5). The peaks observed at 1606 cm⁻¹ and 834
 276 cm⁻¹ may be assigned to $\nu(\text{C=N})$ and $\nu(\text{C=S})$ [37-39].

277 The bands at 1606 cm⁻¹ and 834 cm⁻¹ assigned to $\nu(\text{C=N})$ and $\nu(\text{C=S})$ modes and these bands
 278 shifted towards lower frequency in the spectra of Cd(II) complex (Table-5), which indicated
 279 that coordination takes place through nitrogen of $\nu(\text{C=N})$ group and sulphur of $\nu(\text{C=S})$ group.
 280 At lower frequency the complex exhibited new bands at 540 and 397 cm⁻¹ which further
 281 supported the coordination site $\nu(\text{M-N})$ and $\nu(\text{M-S})$ vibrations.

282

283 **Table-5:** FTIR spectral data of the ligand L³ and its Cd(II) metal complex (in cm⁻¹)

Ligand / Metal Complexes	IR/cm ⁻¹			
	$\nu(\text{C=N})$	$\nu(\text{C=S})$	$\nu(\text{M-N})$	$\nu(\text{M-S})$
Ligand (L ³) C ₉ H ₁₁ N ₃ OS	1606	834	-	-
[Cd(L ³) ₂] [CdC ₁₈ H ₂₂ O ₂ N ₆ S ₂]	1574	821	528	397

284

285 3.5 Characterization by UV-visible Spectra

286 The electronic spectral data for the ligand and their metal complex recorded in DMSO are
287 summarized in Table-6. There are two absorption bands, assigned to $n-\pi^*$ and $\pi-\pi^*$
288 transitions, in the electronic spectrum of the ligand. These transitions are also found in the
289 spectra of the complexes, but they are shifted towards lower and higher frequencies,
290 indicating the coordination of the ligand to the metallic ions [40]. The UV spectra of the
291 ligand shows three absorption bands at 260nm,310nm and 355nm.The first two bands are
292 assigned to $\pi-\pi^*$ transitions of azomethine chromospheres and a benzene ring and the third is
293 assigned to $n-\pi^*$ transition of a lone pair of electrons of an azomethine nitrogen and an
294 antibonding π orbital. The absorption band $n-\pi^*$ at 355 nm due to an imine group in the
295 ligand, whereas for the zinc complex, the same was observed at 390 nm with weak absorption
296 intensity which indicate the coordination of zinc with imine group [41]. The zinc complex
297 shows only the charge transfer transition which can be assigned to charge transfer from the
298 ligand to the metal and vice versa, no d-d transitions are expected for d^{10} Zn(II) complex [42].

299 The UV-Vis absorption spectra of the ligand and complex were recorded after dissolving into
300 DMSO solvent at room temperature. There are two absorption bands, assigned to $n-\pi^*$ and
301 $\pi-\pi^*$ transitions, in the electronic spectrum of the ligand. These transitions are also found in
302 the spectra of the complexes, but they are shifted towards lower and higher frequencies,
303 confirming the coordination of the ligand to the metallic ions [43]. The electronic spectrum of
304 ligand exhibits three intense absorption peaks at 260 nm, 310 nm and 350nm.The first and
305 second peaks were attributed to benzene $\pi-\pi^*$ and imino $\pi-\pi^*$ transitions and the third peak in
306 the spectra was assigned to $n-\pi^*$ transition [44]. The electronic spectra of the Ni(II) complex
307 with an electronic configuration of d^8 shows three new absorption bands in the visible region
308 and these three bands of the transitions $^1A_{1g} \rightarrow ^1A_{2g}$ (355nm), $^1A_{1g} \rightarrow ^1B_{1g}$ (380nm) and
309 $^1A_{1g} \rightarrow ^1E_g$ (420 nm) were observed in the spectra of a square-planar Ni(II) complex [45,46].

310 The UV-Vis absorption spectra of the ligand and complex were recorded after dissolving into
311 DMSO solvent at room temperature. There are two absorption bands, assigned to $n-\pi^*$ and
312 $\pi-\pi^*$ transitions, in the electronic spectrum of the ligand. These transitions are also found in
313 the spectra of the complexes, but the ligand to the metallic ions [47]. The electronic spectrum
314 of ligand exhibits three intense absorption peaks at 260 nm, 310 nm and 350nm. The first and
315 second peaks were attributed to benzene $\pi-\pi^*$ and imino $\pi-\pi^*$ transitions and the third peak in
316 the spectra was assigned to $n-\pi^*$ transition. Due to Forbidden transition, several bands were
317 observed in the visible region of Mn(II) complex, and the band at 430 nm is attributed to (d-
318 d) transition of type $^6A_1 \rightarrow ^4T_2$.

319 The electronic absorption spectra of ligand L¹ and its Sn (II) complex in DMSO solution
 320 were carried out in the range of 200-800 nm at room temperature. There is a shift of the
 321 bands to longer wave length in spectra of complex is a good evidence of complex formation.
 322 There were various bands in the ligand spectra assigned to inter ligand and charge transfer of
 323 n- π^* transitions according to their energies and intensities. Ligand exhibits three intense
 324 absorption peaks at 260 nm, 310 nm and 350nm. The first and second peaks were attributed to
 325 benzene $\pi-\pi^*$ and imino $\pi-\pi^*$ transitions and the third band in the spectra was assigned to n-
 326 π^* transition. The complex showed an intense band at 410nm due to the n- π^* transition of
 327 azomethine chromosphere and the band at 340 nm may be assigned as charge transfer band. It
 328 has been reported that the metal is capable of forming dn-p π^* bonds with ligands containing
 329 nitrogen as the donor atom. The Sn atom has its 5d orbital completely vacant and hence
 330 Sn \leftarrow N bonding can take place by the acceptance of the lone pair of electrons from the
 331 azomethine nitrogen of the ligand [48-50].

332

333 **Table-6:** Magnetic moments and electronic spectral data for ligand (L¹) and its metal
 334 complexes

Compound	λ_{\max} n.m	Wave number cm ⁻¹	μ_{eff} B.M	Assignment
C ₈ H ₉ ON ₃ S	260	38461	-	$\pi \rightarrow \pi^*$
	310	32258		$\pi \rightarrow \pi^*$
	350	38571		n $\rightarrow \pi^*$
[NiC ₁₆ H ₁₆ O ₂ N ₆ S ₂].H ₂ O	355	28169	1.469	¹ A _{1g} \rightarrow ¹ A _{2g}
	380	26315		¹ A _{1g} \rightarrow ¹ B _{1g}
	420	23809		¹ A _{1g} \rightarrow ¹ E _g
[ZnC ₁₆ H ₁₆ O ₂ N ₆ S ₂].2H ₂ O	265	37735	0.5197	C.T (M \rightarrow L)
	320	31250		C.T (M \rightarrow L)
	390	25641		C.T (M \rightarrow L)
[MnC ₁₆ H ₁₆ O ₂ N ₆ S ₂].H ₂ O	325	30769	2.507	⁶ A ₁ \rightarrow ⁴ T ₂
	380	26315		
	430	23255		

335

336 The magnetic moment and electronic spectra are very effective in the evaluation of results
 337 obtained by other methods of structural investigation. Information regarding the geometry of
 338 the complex of Co(II) ions was obtained from electronic spectral studies and magnetic
 339 moments (Table-7). The electronic spectra of ligand and their metal complexes were recorded
 340 in DMSO. Electronic spectrum of ligand shows strong absorption band at 330nm region can
 341 be assigned to the $n \rightarrow \pi^*$ transition of the azomethine group of ligand, which slightly shifted
 342 to lower frequency in the spectra of the complex, indicating that the azomethine nitrogen
 343 atom is involved in coordination to the metal ion. The Co(II) complex was found the
 344 magnetic moment 4.0137 B.M which indicated the three unpaired electrons per Co(II) ion
 345 attaining an octahedral environment [60]. The electronic spectrum of Co(II) complex shows
 346 bands at 264nm and 274nm are assignable to metal-ligand charge transfer band and the band
 347 400nm is assignable to ${}^4T_{1g}(F) \rightarrow {}^4T_{1g}(P)$ transition.

348

349 **Table-7:** The electronic spectral data and magnetic moments for ligand (L^2) and it's metal
 350 complex

Compound	λ_{\max} n.m	Wave number cm^{-1}	μ_{eff} B.M	Assignment
$\text{C}_{14}\text{H}_{11}\text{O}_3\text{N}$	330	30303	-	$n \rightarrow \pi^*$
$[\text{CoC}_{28}\text{H}_{18}\text{O}_6\text{N}_2] \cdot 2\text{H}_2\text{O}$	264	37878	4.0137	Charge transfer(C.T)
	274	36496		C.T (M \rightarrow L)
	400	25000		${}^4T_{1g}(F) \rightarrow {}^4T_{1g}(P)$

351

352 The electronic spectral data for the ligand and it's metal complex recorded in DMSO are
 353 summarized in Table-8. There are two absorption bands, assigned to $n \rightarrow \pi^*$ and $\pi \rightarrow \pi^*$
 354 transitions, in the electronic spectrum of the ligand. These transitions are also found in the
 355 spectra of the complexes, but they are shifted towards lower and higher frequencies,
 356 indicating the coordination of the ligand to the metallic ions. The UV spectra of the ligand
 357 shows three absorption bands at 280nm,330nm and 350nm. The first two bands are assigned
 358 to $\pi \rightarrow \pi^*$ transitions of azomethine chromospheres and a benzene ring and the third is assigned
 359 to $n \rightarrow \pi^*$ transition of a lone pair of electrons of an azomethine nitrogen and an anti-bonding π
 360 orbital. The absorption band $n \rightarrow \pi^*$ at 350nm due to an imine group in the ligand, whereas for

361 the Cd(II) complex, the same was observed at 400 nm with weak absorption intensity which
 362 indicate the coordination of cadmium with imine group. The cadmium complex show only
 363 the charge transfer transition which can be assigned to charge transfer from the ligand to the
 364 metal and vice versa, no d-d transition are expected for diamagnetic d¹⁰ Cd(II) complex. The
 365 shifting of ligand absorption in the UV region, in the spectra of the complex confirming the
 366 coordination of the ligand to metal like Cd (II) ions.

367

368 **Table-8:** Magnetic moments and electronic spectral data for ligand (L³) and it's Cd(II)
 369 Complex

Compound	λ_{\max} n.m	Wave number cm ⁻¹	μ_{eff} B.M	Assignment
C ₉ H ₁₁ N ₃ OS	280	35714	—	$\pi \rightarrow \pi^*$
	330	30303		$\pi \rightarrow \pi^*$
	350	28571		n \rightarrow π^*
[CdC ₁₈ H ₂₂ O ₂ N ₆ S ₂]	295	33898	0.4606	C.T (M \rightarrow L)
	340	29412		C.T (M \rightarrow L)
	400	25000		C.T (M \rightarrow L)

370

371 3.6 Thermogravimetric Analysis

372 3.6.1. Zn(II),Ni(II),Mn(II) and Sn(II) complexes of ligand C₈H₉ON₃S (L¹)

373 The thermal decomposition analysis of solid Zn(II), Ni(II), Mn(II) and Sn(II) metal
 374 complexes were carried out under nitrogen atmosphere and heating rate was suitably
 375 controlled at 30°C min⁻¹ and the weight loss was measured from the ambient temperature up
 376 to 800°C. The data from TGA and DTG clearly indicated that the decomposition of the
 377 complexes proceed in three or four steps. There were some minor steps and asymmetry of
 378 TGA/DTG curves also observed. The weight losses for each complex were calculated within
 379 the corresponding temperature ranges. The different thermodynamic parameters are listed in
 380 Table-9 and the decomposition curves are shown as supplementary materials.

381 The TGA and DTG curve of Zn(II) complex indicated that the complex was decomposed into
 382 four main steps. In the first step of decomposition, two molecules of water were lost at the
 383 temperature range of 85-110°C (calculated 7.36%, experimental 7.20%). In this temperature

384 range the loss of water molecules indicates that the water molecules are of lattice type
385 [51,52]. In the temperature range 130-335°C (calculated 24.00% and experimental 23.10%),
386 the part of ligand-2CSNH₂ were decomposed at the second step. The other part of the ligand
387 2C₆H₄O⁻ were decomposed in third step at 335-740°C (calculated 37.50%, experimental 32
388 .00%). At above 750°C temperature the complex was decomposed and removed as Zn/ZnO
389 (calculated 31.14%, experimental 37.70%) polluted with few carbon atoms [53].

390 The TGA and DTG curve of Ni(II) complex confirmed that the complex was decomposed
391 into four main steps. The 1st step involves the removal of one molecule of hydrated water
392 (calculated 3.87%, experimental 4.00% weight) at temperature range 80-190°C [54,55]. In the
393 2nd step the part of the ligand 2C₆H₄O⁻ was decomposed at 280-350°C (calculated 39.59%,
394 experimental 34.82% weight). At the 3rd step the fragmentation of coordinated ligand
395 2C₂H₄N₃ S was decomposed from the complex at the temperature range 360-750°C
396 (calculated 43.90%, experimental 44.20% weight) and above 750°C temperature the complex
397 was completely decomposed and removed as Ni/NiO (calculated 12.64%, experimental
398 16.98%).

399 In the case of Mn(II) complex the TGA and DTG curve indicated that the complex was
400 decomposed into four main steps. At 1st step one molecule of hydrated water was removed at
401 80-180°C (calculated 3.90%, experimental 4.00%) [54,55]. Then the dehydrated complex was
402 gradually decomposed and the part of ligand 2C₆H₄O⁻ was removed at the temperature range
403 180-350°C (calculated 39.92%, experimental 38.10%). The 3rd step involves the
404 decomposition of the ligand part 2CH₃N₂S at the temperature range 350-770°C (calculated
405 32.54%, experimental 32.22%). At above 770°C temperature finally the complex was
406 completely decomposed and removed as Mn/MnO (calculated 23.64%, experimental
407 25.68%).

408 The Sn(II) complex showed high thermal stability and decomposed above 170 °C, indicating
409 the absence of any lattice water molecules [69]. This complex was decomposed into four
410 main steps. At first step the part of ligand (-2CH₂NS) were decomposed at temperature
411 170-275°C (calculated 23.67%, experimental 22.00%). In 2nd step the decomposition of (-
412 2CHN-) moiety was take place at temperature 275-330°C (calculated 12.0%, experimental
413 10.65 %). The ligand part (2C₆H₄O⁻) were decomposed at the 3rd step at temperature range
414 330-750°C (calculated 36.29%, experimental 36.10 %) and finally the complex was
415 completely decomposed and removed as Sn/SnO (calculated 28.04%, experimental 31.25%).

417 **Table- 9:** Thermal data of Zn(II), Ni(II), Mn(II), Sn(II), Cd(II) and Co(II) complexes.

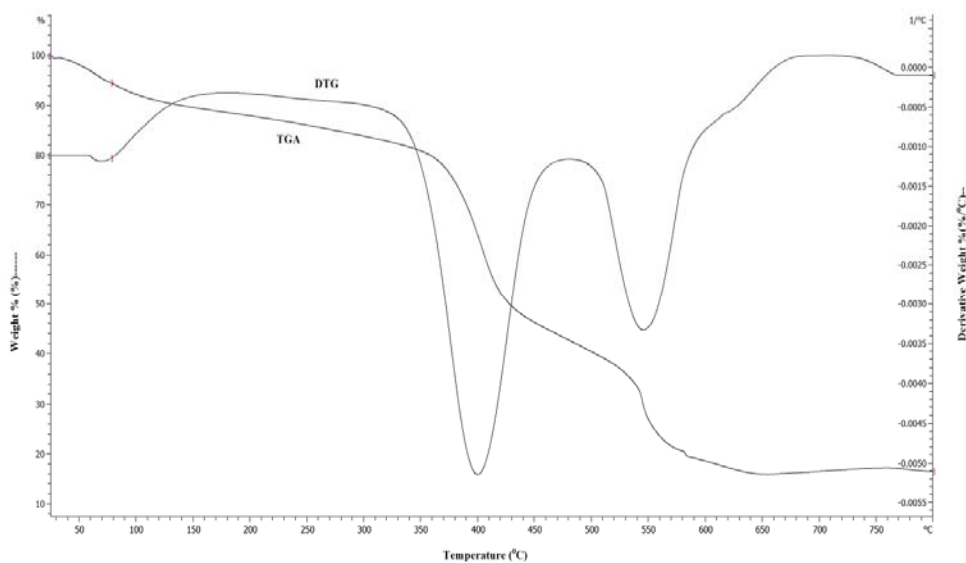
Complexes	Steps	Temperature Range/ °C	DTG Peak/ °C	TG mass loss% calc./found	Assignments
[ZnC ₁₆ H ₁₆ O ₂ N ₆ S ₂].2H ₂ O	1 st	85-110	97	7.36/7.20	2H ₂ O
	2 nd	130-335	278	24.00/23.10	2CSNH ₂
	3 rd	335-740	350	37.50/32.00	2C ₆ H ₄ O-
	4 th	>750		31.14/37.7	Zn/ZnO
[NiC ₁₆ H ₁₆ O ₂ N ₆ S ₂].H ₂ O	1 st	80-190	180	3.87/4.00	H ₂ O
	2 nd	280-350	295	39.59/34.82	2C ₆ H ₄ O ⁻
	3 rd	360-750	382	43.90/44.20	2C ₂ H ₄ N ₃ S
	4 th	>750		12.64/16.98	Ni/NiO
[MnC ₁₆ H ₁₆ O ₂ N ₆ S ₂].H ₂ O	1 st	80-180	118	3.90/4.00	H ₂ O
	2 nd	180-350	290	39.92/38.10	2C ₆ H ₄ O ⁻
	3 rd	350-770		32.54/32.22	2CH ₃ N ₂ S
	4 th	>770		23.64/25.68	Mn/MnO
[SnC ₁₆ H ₁₆ O ₂ N ₆ S ₂]	1 st	170-275	240	23.67/22.00	2CH ₂ NS
	2 nd	275-330	290	12.00/10.65	2CHN-
	3 rd	330-750	370	36.29/36.10	2C ₆ H ₄ O ⁻
	4 th	>750		28.04/31.25	Sn/SnO
[CoC ₂₈ H ₁₈ O ₆ N ₂].2H ₂ O	1 st	40-110	65	6.28/6.32	2H ₂ O
	2 nd	110-480	400	51.31/49.20	2C ₈ H ₅ O ₂ N
	3 rd	480-650	548	32.12/28.80	2C ₆ H ₄ O ⁻
	4 th	>650		10.29/15.72	Co/CoO
[CdC ₁₈ H ₂₂ O ₂ N ₆ S ₂]	1 st	230-455	282	50.53/49.23	2C ₈ H ₈ ON
	2 nd	455-740	570	28.28/27.05	2CH ₃ N ₂ S
	3 rd	>740		21.19/24.00	Cd/CdO

418

419 **3.6.2. Co(II) complex of ligand C₁₄H₁₁O₃N (L²)**

420 TGA was carried out for solid Co(II) metal complex under N₂ flow. The heating rate was
 421 suitably controlled at 30°C min⁻¹ and the weight loss was measured from the ambient

422 temperature up to 800°C. The thermogram of complex exhibits three clear cut decomposition
 423 stages in (figure-3). The first stage with estimated mass loss of 6.32% (calculated mass loss
 424 6.28%) within the temperature range 40–110°C corresponding to the loss of water molecules
 425 [56,57]. The second stage occurs at 110–480°C, with a mass loss of 49.20% (calculated
 426 51.31%) , corresponding to the loss of 2C₈H₅O₂N parts of the ligand. The third stage of
 427 decomposition occurs at the temperature range 480–650°C, with a mass loss of 28.80%
 428 (calculated 32.12%), corresponding to the loss of 2C₆H₄O moiety. At above 650°C
 429 temperature the complex was completely decomposed and removed as of 15.72% (calculated
 430 10.29%). The different TG and DTG data are given in Table-9.



431

432 Figure-3: TGA and DTG curve of [CoC₂₈H₁₈O₆N₂].2H₂O

433

434 3.6.3. Cd(II) complex of ligand C₉H₁₁N₃OS (L³)

435 Thermogravimetric analysis of solid Cd(II) metal complex under N₂ flow. The heating rate
 436 was suitably controlled at 30°C min⁻¹ and the weight loss was measured from the ambient
 437 temperature up to 800°C. The TGA curve of the Cd(II) complex showed no mass loss up to
 438 230 °C, indicating the absence of lattice / coordinated water [58,59] and the high thermal
 439 stability of the complex. The thermogram of Cd(II) complex is given in Fig.4.24, which
 440 shows two stage decomposition pattern. The first stage was exhibited a maximum mass loss
 441 of 49.23% (calculated 50.53%) of ligand part (2C₈H₈ON) at 230-455°C. The second stage

442 occurs at 455–740°C, with a mass loss of 27.05% (calculated 28.28%) attributed to the loss
 443 of (2CH₃N₂S) moiety. Finally at above 750°C temperature the complex was completely
 444 decomposed and removed as Cd/CdO of 24.0% (calculated 21.19%). The different TG and
 445 DTG data are given in Table-9.

446 3.6.4. Antibacterial activity

447 The prime objective of performing the antibacterial screening is to determine the
 448 susceptibility of the pathogenic microorganism to test the compound which, in turn is used to
 449 selection of the compound as a therapeutic agent. The free Schiff base ligand and their metal
 450 complexes were screened for their antibacterial activity against strains the *Bacillus cereus*
 451 *ATCC25923*, *Streptococcus agelactiae*, *Escherichia coli ATCC 25922*, *Shigella dysenteriae*
 452 The compounds were tested at a concentration of 30 µg/0.01 mL in DMSO solution using the
 453 paper disc diffusion method with Kanamycin as standard. The susceptibility zones were
 454 measured in diameter (mm) and the result are listed in Table-10. The susceptibility zones
 455 were the clear zones around the discs killing the bacteria.

456

457 **Table 10.** Antibacterial activities of the complexes.

Bacterials strains	Zone of inhibition, diameter in mm						
	A (10µg /disc)	B (10µg /disc)	C (10µg /disc)	D (10µg /disc)	E (10µg /disc)	F (10µg /disc)	K (30µg /disc)
Gram positive							
<i>Bacillus cereus</i>	22	10	19	12	11	14	36
<i>Streptococcus agelactiae</i>	19	09	21	08	14	16	35
Gram negative							
<i>Escherichia coli</i>	23	12	24	09	12	18	32

<i>Shigella</i>	09	11	10	12	08	14	36
<i>dysenteriae</i>							

458

459 Where, A = $[C_{16}H_{16}ZnO_2N_6S_2].2H_2O$, B = $[C_{16}H_{16}NiO_2N_6S_2].H_2O$, C = $[C_{16}H_{16}MnO_2N_6S_2].H_2O$, D =
 460 $[C_{16}H_{16}SnO_2N_6S_2]$, E = $[C_{28}H_{18}CoO_6N_2].2H_2O$, F = $[C_{18}H_{22}CdO_2N_6S_2]$ and K = Kanamycin

461 4. Conclusions

462 In this paper we have explored the synthesis and coordination Chemistry of Ni(II), Zn(II),
 463 Mn(II), Sn(II), Co(II) and Cd(II) ions were synthesized with three different synthesized
 464 Schiff base ligands viz (L¹) [2-(2-hydroxybenzylidene)hydrazinecarbothioamide, (L²) [4-((4-
 465 hydroxybenzylidene)amino)benzoic acid and (L³) [2-(4-
 466 methoxybenzylidene)hydrazinecarbothioamide]. The ligands and metal complexes were
 467 characterized by molar conductivity measurement, magnetic susceptibility, Infrared,
 468 electronic spectral, thermal analysis and some physical measurements. The overall reactions
 469 were monitored by TLC analysis. Molar conductance study have shown that all the
 470 complexes were non electrolytic in nature. FTIR studies suggested that Schiff bases act as
 471 deprotonated bidentate ligands and metal ions are attached with the ligands-(L¹), (L²) by N, O
 472 and ligand-(L³) by N, S coordinating sites during complexation reaction. Magnetic
 473 susceptibility data coupled with electronic spectra revealed that $[ZnC_{16}H_{16}O_2N_6S_2].2H_2O$,
 474 $[MnC_{16}H_{16}O_2N_6S_2].H_2O$, $[SnC_{16}H_{16}O_2N_6S_2]$ and $[CdC_{18}H_{22}O_2N_6S_2]$ complexes have tetrahedral,
 475 $[NiC_{16}H_{16}O_2N_6S_2].H_2O$ has square planer and $[CoC_{28}H_{18}O_6N_2].2H_2O$ has octahedral geometry.
 476 Thermal analysis (TGA and DTG) data showed the possible degradation pathway of the
 477 complexes and also indicated that most of the complexes were thermally stable up to 200⁰C.
 478 The Schiff bases and their metal complexes have been found moderate to strong
 479 antimicrobial activity.

480

481 REFERENCES

482 [1]. Angela Kriza, Lucica Viorica Ababei, Nicoleta Cioatera, Ileana Rău And Nicolae
 483 Stănică, Synthesis And Structural Studies Of Complexes Of Cu, Co, Ni And Zn With
 484 Isonicotinic Acid Hydrazide And Isonicotinic Acid (1-Naphthylmethylene)Hydrazide,
 485 J. Serb. Chem. Soc., 2010;75 (2):229- 242.

- 486 [2]. P. K. Das, N. Panda, N. K. Behera, Synthesis, Characterization and Antimicrobial
487 Activities of Schiff Base Complexes Derived from Isoniazid and Diacetylmonoxime,
488 IJSET – Int. J. of Innovative Sci., Eng. & Tech., 2016;3(1): 42-54.
- 489 [3]. Anil Kumar M R, Shanmukhappa S, Rangaswamy B E, Revanasiddappa M,
490 Synthesis, Characterization, Antimicrobial Activity, Antifungal Activity and DNA
491 Cleavage Studies of Transition Metal Complexes with Schiff Base Ligand, Int. J. of
492 Innovative Sci., Eng. & Tech., 2015;4(2): 60-66.
- 493 [4]. O' Boyle N M, Tenderholt A L & Langer K M, cclib: a library for package-
494 independent computational chemistry algorithms J. Comput. Chem., 2008; 29:839.
- 495 [5]. Saud I. Al-Resayes, Mohammad Shakir, Ambreen Abbasi, Kr. Mohammad Yusuf
496 Amin, Abdul Lateef, Synthesis, spectroscopic characterization and biological
497 activities of N4O2 Schiff base ligand and its metal complexes of Co(II), Ni(II), Cu(II)
498 and Zn(II), Spectromica Acta Part A , 2012; 93:86-94.
- 499 [6]. K.D. Karlin, Z. Tyeklar, Bioinorganic Chemistry of Copper, Chapman & Hall: New
500 York, 1993;101-109.
- 501 [7]. V. Arun, N. Sridevi, P.P. Robinson, S. Manju, K.K.M. Yusuff, “Ni(II) and Ru(II)
502 Schiff base complexes as catalysts for the reduction of benzene” J. Mol. Catal. A:
503 Chem., 2009; 304 (1-2):191-198.
- 504 [8]. K. C. Gupta, A. K. Sutar, Catalytic activities of Schiff base transition metal
505 complexes, Coord. Chem. Rev., 2008; 252 (12-14):1420-1450.
- 506 [9]. R. I. Kureshy, N. H. Khan, S. H. R. Abdi, P. Iyer and S. T. Patel ,Chiral Ru(II) Schiff
507 base complexes catalysed enantio selective epoxidation of styrene derivatives using
508 iodosyl benzene as oxidant II, J. Mol. Catal., 1999;150(1-2):175-183.
- 509 [10]. Saud I. Al-Resayes, Mohammad Shakirb, Ambreen Abbasi, Kr. Mohammad Yusuf
510 Amin, Abdul Lateef, Spectromica Act.a Part A, 2012;93:86-94.
- 511 [11]. Rakesh Ranjan and Dhanashree S Hallooman, Synthesis And Characterization Of
512 Co(Ii) And Ni(Ii) Complexes With Schiff Base 2,2-
513 Dimethylpropiophenonethiosemicarbazone, Int. J. of Res. In Pharm. And Chem.,
514 2014;4(2):423-426.
- 515 [12]. Angela Kriza, Mariana Loredana Dianu, Nicolae Stănică, Constantin Drăghici, Mona
516 Popoiu, Synthesis and Characterization of Some Transition Metals Complexes with
517 Glyoxalbis- Isonicotinoyl Hydrazone, 2009;60(6):555-560.

- 518 [13]. L. Mitu, A. Kriza, Synthesis and Characterization of Complexes of Mn(II), Co(II),
519 Ni(II) and Cu(II) with an Aroylhydrazone Ligand. *Asian J. Chem.*, 2007;19 (1):658-
520 664.
- 521 [14]. Ljubijankić N., Tešević V., Grgurić-Šipka S., Jadranin M., Begić S., Buljubašić L.,
522 Markotić E., Ljubijankić S., Synthesis and characterization of Ru(III) complexes with
523 thiosemicarbazide-based ligands, 2016;47:1-6.
- 524 [15]. Methak. S. Mohammad, Preparation and Characterization of Some Transition Metal
525 Complexes with Schiff base of thiosemicarbazone, *J. of Kerbala Uni., Scien.* 2010;8
526 (1):8-17 .
- 527 [16]. R.V. Singh, N. Fahmi and M.K. Biyala, Coordination Behavior and Biopotency of N
528 and S/O Donor Ligands with their Palladium(II) and Platinum(II) Complexes, *J. of the*
529 *Ir. Chem. Soc.*, 2005;2(1):40-46.
- 530 [17]. A. M. Vijey, G. Shiny, and V. Vaidhyalingam, Synthesis and antimicrobial activities
531 of 1-(5-substituted-2-oxo indolin-3-ylidene)-4-(substituted pyridin-2-yl)
532 thiosemicarbazide, *Arkivoc (xi)*., 2008;187.
- 533 [18]. Mohammad Asif, A Review On Biological Activities Of Benzimidazole, Oxadiazole
534 And Mannich Base Derivatives Of Benzimidazole-Oxadiazole Merged Compounds,
535 *Int. J. of Cur. Res. in App. Chem. & Chem. Eng.*, 2017;3(1):20-29.
- 536 [19]. M. M. H. Khalil, M. M. Aboaly and R. M. Ramadan, Spectroscopic and
537 electrochemical studies of ruthenium and osmium complexes of salicylideneimine-2-
538 thiophenol Schiff base, *Spectrochimica Acta Part A: Mol. and Bio. Spec...*,
539 2005;61(1):157-161.
- 540 [20]. P. M. Dahikar, R. M. Kedar, Synthesis, spectral and biological activity of transition
541 metal complexes of substituted benzoine semicarbazones, *Inter. J. of Appl. or Inn. in*
542 *Engg. & Man. (IJAIEEM)*, 2013;2(4):8-11.
- 543 [21]. P. Murali Krishna, B. S. Shankara, and N. Shashidhar Reddy, Synthesis,
544 Characterization, and Biological Studies of Binuclear Copper(II) Complexes of (2E)-
545 2-(2-Hydroxy-3-Methoxybenzylidene)-4N-Substituted Hydrazine carbothioamides,
546 Hindawi Publishing Corporation, *International Journal of Inorganic Chemistry*,
547 2013,11pages.
- 548 [22]. Ljiljana S. Vojinović-Ješić, Vukadin M. Leovac, Mirjana M. Lalović, Valerija I.
549 Češljević, Ljiljana S. Jovanović, Marko V. Rodić and Vladimir Divjaković, Transition
550 metal complexes with thiosemicarbazide-based ligands. Part 58. Synthesis, spectral

- 551 and structural characterization of dioxovanadium(V) complexes with
552 salicylaldehydethiosemicarbazone, *J. Serb. Chem. Soc.* 2011;76 (6):865–877.
- 553 [23]. Monika Tyagi, Sulekh Chandra, Synthesis, characterization and biocidal properties of
554 platinum metal complexes derived from 2,6-diacetylpyridine (bisthiosemicarbazone),
555 *Open Jo. of Inorg. Chem.*, 2012;2:41-48.
- 556 [24]. Vojinović-Ješić L.J. S., Leovac V.M., Lalović M. M., Češljević V.I., Jovanović
557 Lj.S. Rodić M. V. and Divjaković V, Transition metal complexes with
558 thiosemicarbazide-based ligands. Part 58. Synthesis, spectral and structural
559 characterization of dioxovanadium(V) complexes with salicyl aldehyde
560 thiosemicarbazone, *J. Serb. Chem. Soc.*, 2011;76 (6):865–877.
- 561 [25]. Baiu S.H., El-Ajaily M.M. and El-Barasi, Antibacterial Activity of Schiff Base
562 Chelates of Divalent Metal Ions, *Asian Journal of Chemistry*, (2009);21(1):5-10.
- 563 [26]. Elena Pahontu, Valeriu Fala, Aurelian Gulea, Donald Poirier, Victor Tapcov and
564 Tudor Rosu, Synthesis and Characterization of Some New Cu(II), Ni(II) and Zn(II)
565 Complexes with Salicylidene Thiosemicarbazones: Antibacterial, Antifungal and in
566 Vitro Antileukemia Activity, *Molecules*, 2013;18:8812-8836.
- 567 [27]. El-Bahnasawy R. M., Sharaf El-Deen L.M., El-Table A.S., Wahba M. A. and El-
568 Monsef. A., Electrical Conductivity Of Salicylaldehyde Thiosemicarbazone and its
569 Pd(II), Cu(II) and Ru(III) Complexes, *Eur. Chem. Bull*, 2014;3(5):441-446.
- 570 [28]. Md. Saddam Hossain, C.M. Zakaria, M.M. Haque, and Md. Kudrat-E-Zahan, Spectral
571 and thermal characterization with antimicrobial activity on Cr(III) and Sn(II)
572 Complexes containing N,O Donor novel schiff base ligand, *Int. J. of Chem. Studies.*,
573 2016;4(6):08-11.
- 574 [29]. A. Xavier, P. Gopu, B. Akila, K. Suganya, Synthesis and Characterization of Schiff
575 Base from 3, 5-Di Chloro Salicylaldehyde with 4-Bromoaniline and 4-Aminobenzoic
576 Acid and Its 1st Row Transition Metal Complexes, *Int. J. of Inn. Res. & Dev.*,
577 2015;4(8):384-396.
- 578 [30]. Manohar V. Lokhande and Mrityunjay R. Choudhary, Some Transitional Metal Ions
579 Complexes With 3-[(E)-(4-Fluorophenyl) Methylidene] Amino} Benzoic Acid And
580 Its Microbial Activity, *International Journal of Pharmaceutical Sciences and
581 Research, IJPSR*, 2014;5(5):1757-1766.
- 582 [31]. P. Gopu, Dr. A. Xavier, Synthesis and Characterization of 4-(3-bromo-5-chloro-2-
583 hydroxybenzylidene) Benzoic Acid and its Transition Metal Complexes,
584 *International Journal of Science and Research (IJSR)*, 2015;4(8):15-21.

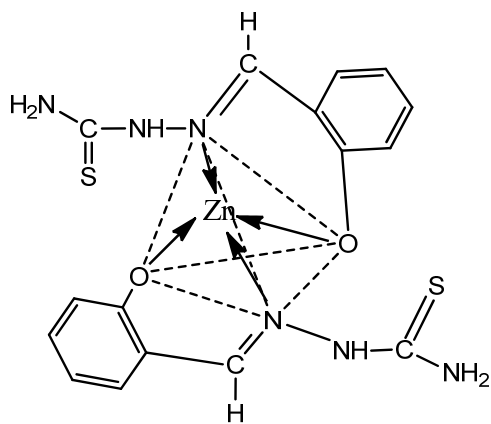
- 585 [32]. Shanker K, Rohini R, Ravinder V and Reddy P M: Ru(II) complexes of N₄ and N₂O₂
586 macrocyclic Schiff base ligands: Their antibacterial and antifungal studies, *Spectro*
587 *chimica Acta A*, 2009;73:1205-211.
- 588 [33]. Raju Ashokan, Saravanan Sathishkumar, Ekamparam Akila And Rangappan Rajavel,
589 Synthesis, Characterization and Biological Activity of Schiff Base Metal Complexes
590 Derived from 2, 4-Dihydroxyacetophenone, *Chemical Science Transactions* , 2017;
591 6(2):277-287 .
- 592 [34]. Miguel-Angel Munoz-Hernandes, Michal L. Mckee, Timothy S. Keizer, Burt C.
593 Yearwood and David Atwood, Six-coordinate aluminiumcations: characterization,
594 catalysis, and theory, 2002;3.
- 595 [35]. K. Nakamoto: *Infrared Spectra of Inorganic and Coordination Compounds*. John
596 Wiley & Sons, New York, 2nd Edition, 1970.
- 597 [36]. Shanker K B, Rohini M, Ravinder Reddy P and Ho M Y P: Synthesis of Tetraaza
598 Macrocyclic Pd(II) complexes; Antibacterial & Catalytic studies, *J.of the Ind. Chem.*
599 *Soc.* 2009, 86.
- 600 [37]. K.P. Satheesh, V. Suryanarayana Rao, Spectrophotometric Method For The
601 Determination Of Trace Amount Of Tungsten (Vi) In Alloy Samples Using 4-
602 Hydroxybenzaldehydethiosemicarbazone, *J. of Adv. Scien. Res.*, 2015; 6(2): 14-17.
- 603 [38]. S. Janarthanan, Y.C. Rajan, P.R. Umarani, D. Jayaraman, D. Premanand and S. Pandi,
604 Synthesis, growth, optical and thermal properties of a new organic crystal
605 semicarbazone of p-anisaldehyde, (SPAS), 2010;3(8):42-47.
- 606 [39]. Ruchi Agarwal, Mohd. Asif Khan and Shamim Ahmad, Schiff base complexes
607 derived from thiosemicarbazone, synthesis characterization and their biological
608 activity , *Journal of Chemical and Pharmaceutical Research*, 2013;5(10):240-245.
- 609 [40]. Sandra S. Konstantinovi, Blaga C. Radovanovi, IvojinCaki And VesnaVasi, Synthesis
610 and characterization of Co(II), Ni(II), Cu(II) and Zn(II) complexes with 3-
611 salicylidenehydrazono-2-indolinone,*J.Serb.Chem.Soc.*, 2003;68(8-9):641-647.
- 612 [41]. N. K. Gondia, J. Priya, S. K. Sharma, Synthesis and physico-chemical
613 characterization of a Schiff base and its zinc complex, *Res Chem Intermed*,
614 2017;43:1165-1178.
- 615 [42]. Lotf A. Saghatforoush, Ali Aminkhani, Sohrab Ershad, Ghasem Karimnezhad,
616 Shahriar Ghammamy and Roya Kabiri, Preparation of Zinc (II) and Cadmium (II)
617 Complexes of the Tetradentate Schiff Base Ligand 2-((E)-(2-(2(pyridine-2-yl)-

- 618 ethylthio)ethylimino)methyl)-4-bromophenol (PytBrsalH), *Molecules* 2008;13:804-
619 811.
- 620 [43]. Jian-Ning Liu, Bo-Wan Wu, Bing Zhang, Yongchun Liu, Synthesis and
621 Characterization of Metal Complexes of Cu(II), Ni(II), Zn(II), Co(II), Mn(II) and
622 Cd(II) with Tetradentate Schiff Bases, *Turk J Chem.*, 2006;30:41-48.
- 623 [44]. Shayma A. Shaker, Preparation and Spectral Properties of Mixed-Ligand Complexes
624 of VO(IV), Ni(II), Zn(II), Pd(II), Cd(II) and Pb(II) with Dimethylglyoxime and N-
625 Acetyl glycine, *E-Journal of Chemistry*, 2010;7(S1):S580-S586.
- 626 [45]. Md. Kudrat-E-Zahan, M. S. Islam, and Md. Abul Bashar ,Synthesis, Characteristics,
627 and Antimicrobial Activity of Some Complexes of Mn(II), Fe(III) Co(II), Ni(II),
628 Cu(II), and Sb(III) Containing Bidentate Schiff Base of SMDTC, *Russian Journal of*
629 *General Chemistry*, 2015;85(3):667–672.
- 630 [46]. Rehab K. Al-Shemary, Ahmed T. Numanand Eman Mutar Atiyah, Synthesis,
631 Characterization And Antimicrobial Evaluation Of Mixed Ligand Complexes Of
632 Manganese(Ii), Cobalt(Ii), Copper(Ii), Nickel(Ii) And Mercury(Ii) With 1,10-
633 Phenanthroline And A Bidentate Schiff Base, *Eur. Chem. Bull.*, 2016;5(8):335-338.
- 634 [47]. Iniama, G.E., Olarele, O.S. and Johnson, A, Synthesis, spectral, characterization and
635 antimicrobial activity of manganese (II) and copper (II) complexes of
636 Salicylaldehydephenylhydrazone, *Int. J. of Chem. and Appl.*, 2015;7(1):15-23.
- 637 [48]. Neelofar, Nauman Ali, Shabir Ahmad, Naser M. Abdel-Salam, Riaz Ullah, Robila
638 Nawaz and Sohail Ahmad, Synthesis and evaluation of antioxidant and antimicrobial
639 activities of Schiff base tin (II) complexes, *Tropical Journal of I Pharmaceutical*
640 *Research* ,2016;15(12):2693-2700.
- 641 [49]. Har Lal Singh and J. B. Singh, Synthesis and Characterization of New Lead(II)and
642 Organotin(IV) Complexes of Schiff Bases Derived from Histidine and Methionine,
643 Hindawi Publishing Corporation, *International Journal of Inorganic Chemistry*,
644 2012,7pages.
- 645 [50]. Sunita Bhanuka and Har Lal Singh, Spectral, Dft And Antibacterial Studies Of Tin(Ii)
646 Complexes Of Schiff Bases Derived From Aromatic Aldehyde And Amino Acids,
647 *Rasayan J. Chem.*, 2017; 10(2):673-68.
- 648 [51]. Khalil Abid, Sinann Al-Bayati, Anaam Rasheed, Synthesis, Characterization,
649 Thermal study and Biological Evaluation of Transition Metal Complexes Supported
650 by ONNNO-Pentadentate Schiff Base Ligand, *American Journal of Chemistry*,
651 2016;6(1):1-7.

- 652 [52]. Allan J. R. and Veitch P. M., The preparation, characterization and thermal analysis
653 studies on complexes of cobalt(II) with 2-, 3-, 4-cyanopyridines, *J. Thermal Anal.*,
654 1983; **27(1): 3-15**.
- 655 [53]. Moamen S. Refat, I. M. El-Deen, M. S. El-Garib, and W. Abd El-Fattah,
656 Spectroscopic and Anticancer Studies on New Synthesized Copper(II) and
657 Manganese(II) Complexes with 1,2,4- Triazines Thiosemicarbazide1, *Russian J. of*
658 *Gen. Chem.*, 2015;85(3): 692–707.
- 659 [54]. Md. Saddam Hossain, Md. Ashraful Islam, C. M. Zakaria, M. M. Haque, Md. Abdul
660 Mannan, Md. Kudrat-E-Zahan, Synthesis, Spectral and Thermal Characterization with
661 Antimicrobial Studies on Mn(II), Fe(II), Co(II) and Sn(II) Complexes of Tridentate
662 N,O Coordinating Novel Schiff Base Ligand” *J. Chem. Bio. Phy. Sci. Sec. A.*, 2016;6
663 (1):041-052.
- 664 [55]. M. R. Islam, J. A. Shampa, M. Kudrat-E-Zahan, M. M. Haque, Y. Reza, Investigation
665 on Spectroscopic, Thermal and Antimicrobial Activity of Newly Synthesized
666 Binuclear Cr(III) Metal Ion Complex , *J. Sci. Res.*, 2016;8 (2):181-189.
- 667 [56]. Sayed M. Abdallah, M.A. Zayed, Gehad G. Mohamed, Synthesis and spectroscopic
668 characterization of new tetradentate Schiff base and its coordination compounds of
669 NOON donor atoms and their antibacterial and antifungal activity, *Arabian J. of*
670 *Chem.*, 2010; 3:103–113.
- 671 [57]. Samir Alghool. Mononuclear complexes based on reduced Schiff base derived fromL-
672 methionine, synthesis, characterization, thermal and in vitro antimicrobial studies, *J*
673 *Therm Anal Calorim*, 2015; 12: 1309–1319.
- 674 [58]. Achut S. Munde, Amarnath N. Jagdale, Sarika M. Jadhav And Trimbak K.
675 Chondhekar, Synthesis, characterization and thermal study of some transition metal
676 complexes of an asymmetrical tetradentate Schiff base ligand, *J. Serb. Chem. Soc.*,
677 2010;75(3):349–359.
- 678 [59]. A.S. Munde, V. A. Shelke, S. M. Jadhav, A. S. Kirdant, S. R. Vaidya, S. G.
679 Shankarwar, and T. K. Chondhekar, Synthesis, Characterization and Antimicrobial
680 Activities of some Transition Metal Complexes of Biologically Active Asymmetrical
681 Tetradentate Ligands, *Adv. Appl. Sci. Res.*, 2012; 3(1):175-182.

682

683 **Supplementary Materials**

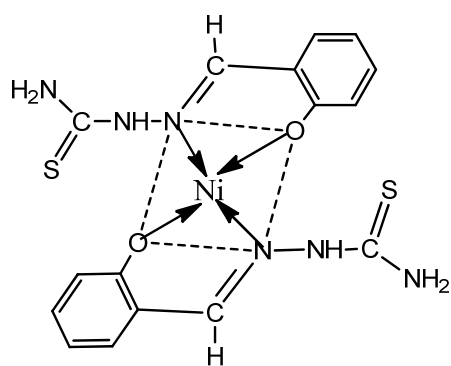


684

685

Figure: Structure of $[C_{16}H_{16}ZnO_2N_6S_2]$

686

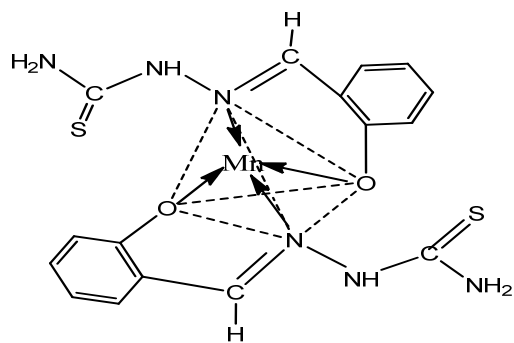


687

688

Figure: Structure of $[C_{16}H_{16}NiO_2N_6S_2]$

689

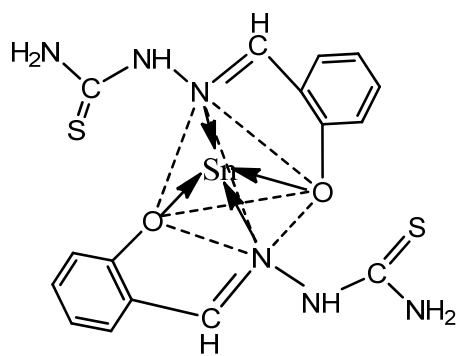


690

691

Figure: Structure of $[C_{16}H_{16}MnO_2N_6S_2]$

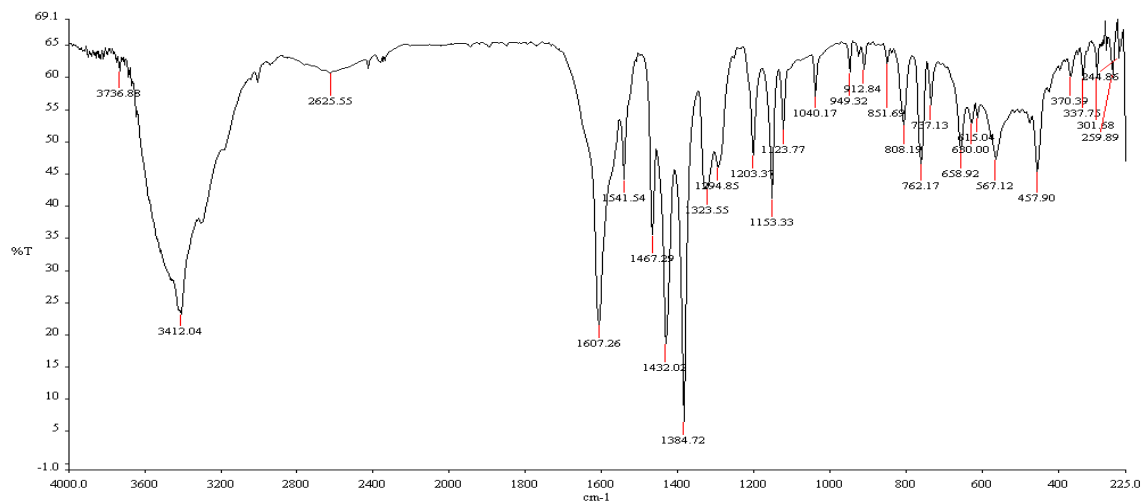
692



693

694

Figure: Structure of $[C_{16}H_{16}SnO_2N_6S_2]$



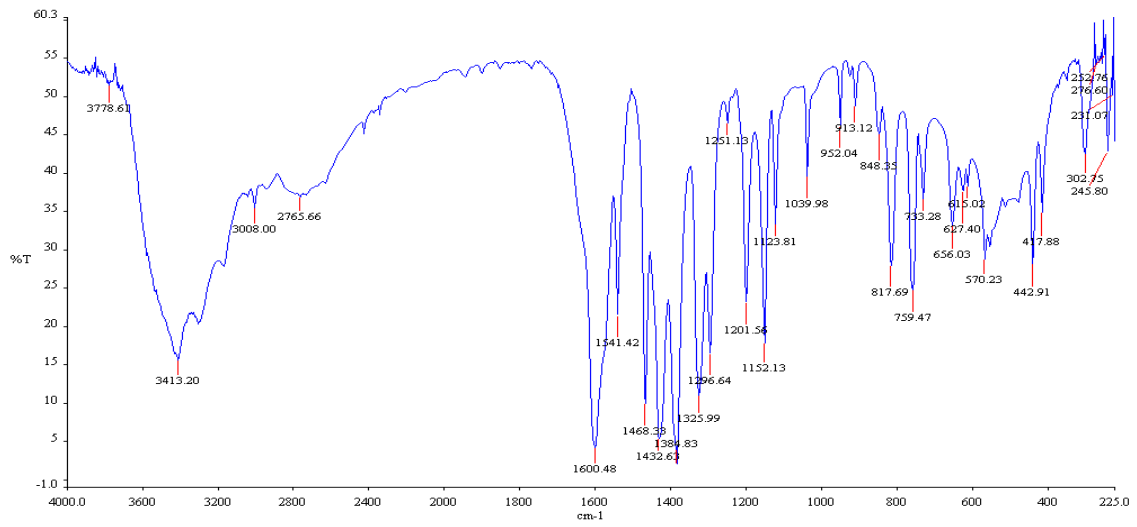
695

696

697

Figure: IR spectra of $[NiC_{16}H_{16}O_2N_6S_2] \cdot H_2O$

698

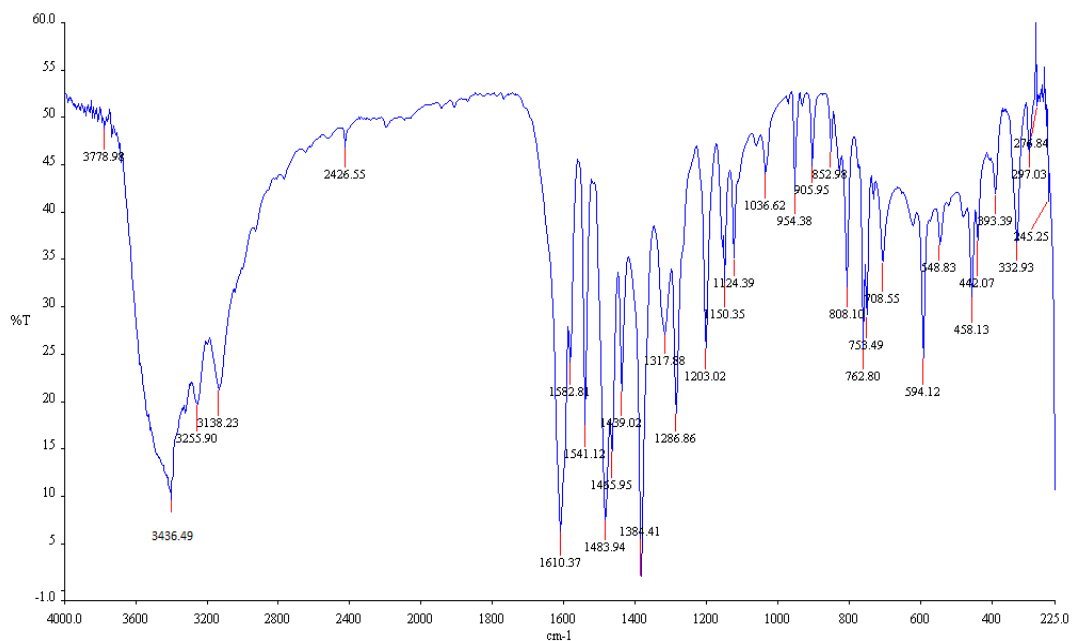


699

700

Figure: IR spectra of $[\text{MnC}_{16}\text{H}_{16}\text{O}_2\text{N}_6\text{S}_2]\cdot\text{H}_2\text{O}$

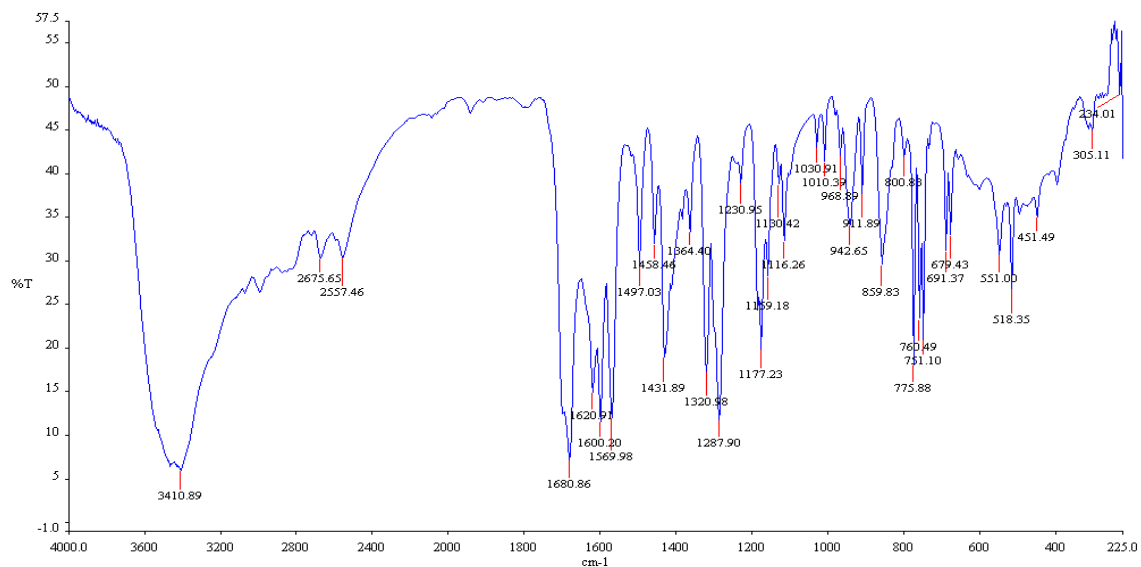
701



702

703

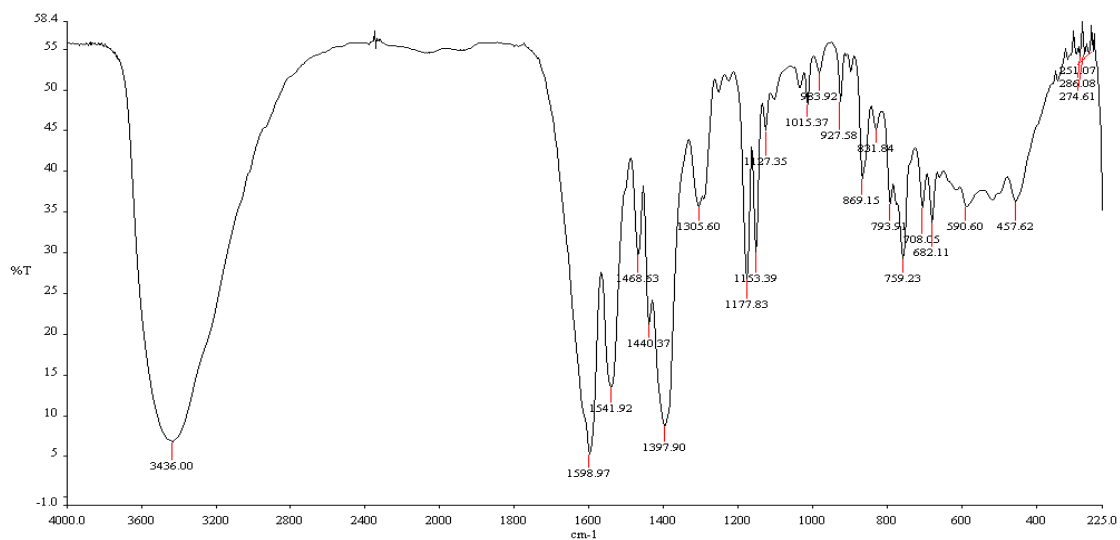
Figure: IR spectra of [SnC₁₆H₁₆O₂N₆S₂]



704

705

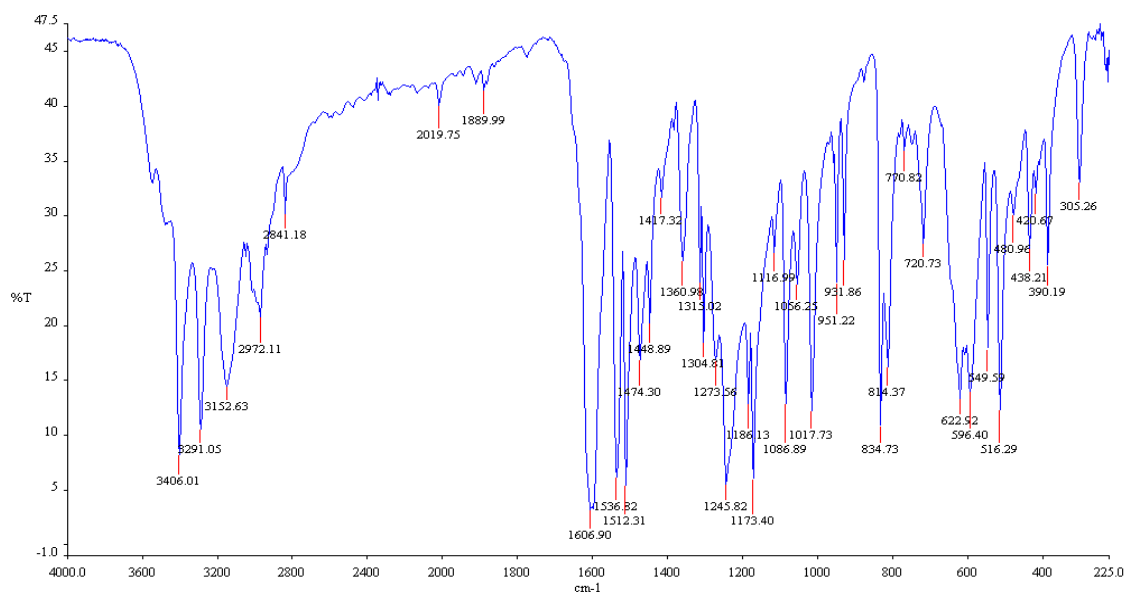
Figure: IR Spectra of 4-((hydroxybenzylidene)amino)benzoic acid ligand(L²)



706

707

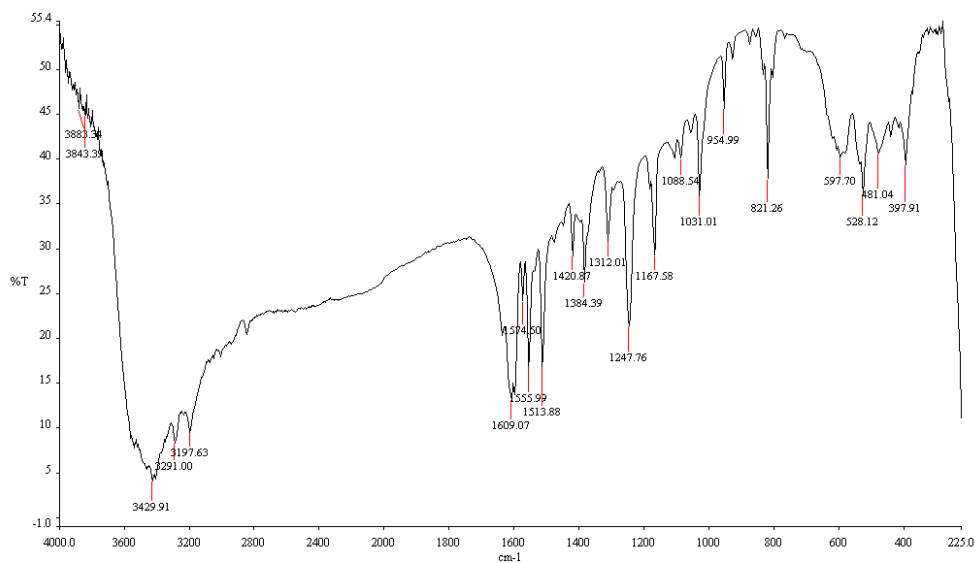
Figure: IR Spectra of $[CoC_{28}H_{18}O_6N_2] \cdot 2H_2O$ with ligand (L^2)



708

709

Figure: IR Spectra of Schiff base ligand $C_9H_{11}N_3OS$ (L^3)

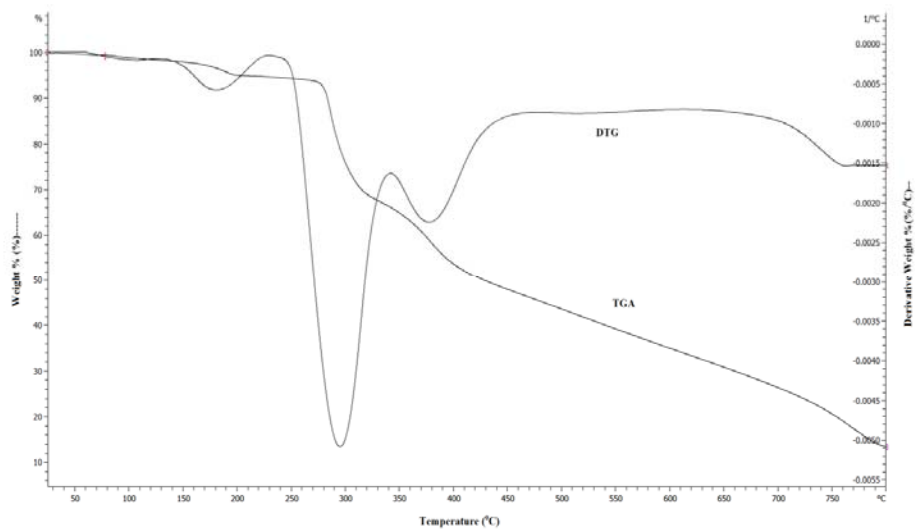


710

Figure: IR Spectra of $[\text{CdC}_{18}\text{H}_{22}\text{O}_2\text{N}_6\text{S}_2]$

711

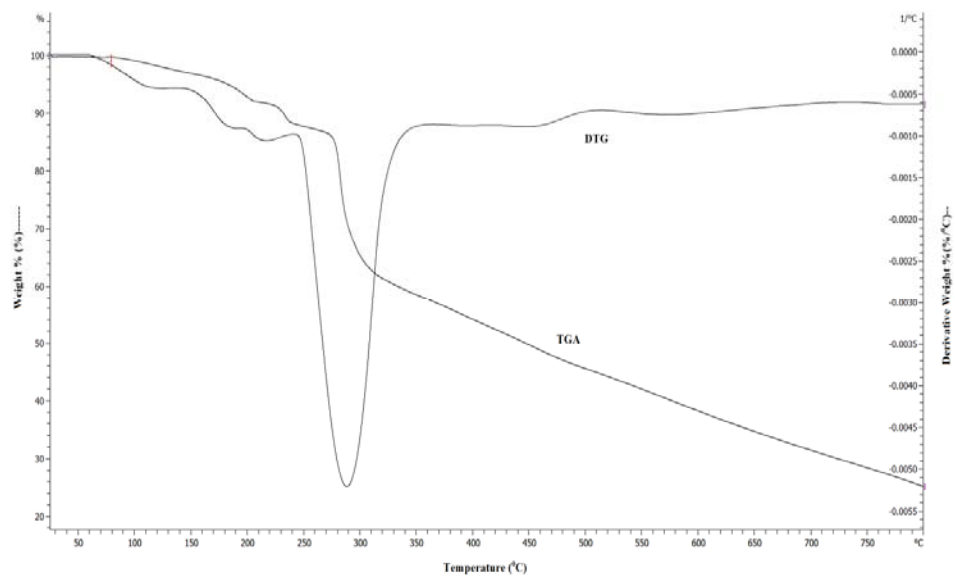
712



713

Figure: TGA and DTG curve of $[\text{NiC}_{16}\text{H}_{16}\text{O}_2\text{N}_6\text{S}_2] \cdot \text{H}_2\text{O}$

714

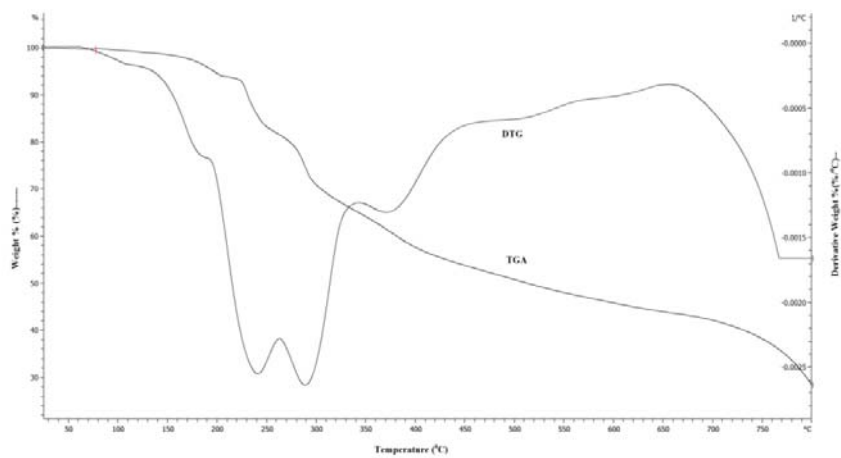


715

Figure: TGA and DTG curve of $[\text{MnC}_{16}\text{H}_{16}\text{O}_2\text{N}_6\text{S}_2]\cdot\text{H}_2\text{O}$

716

717

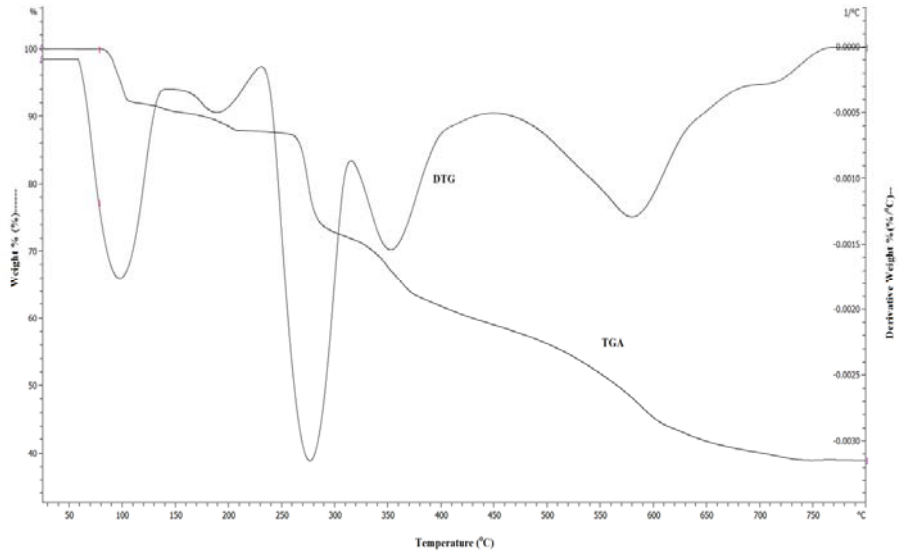


718

Figure: TGA and DTG curve of $[\text{SnC}_{16}\text{H}_{16}\text{O}_2\text{N}_6\text{S}_2]$

719

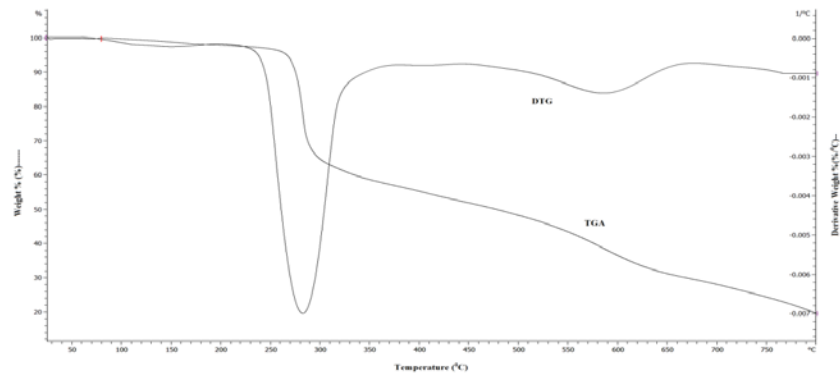
720



721

722

Figure: TGA and DTG curve of $[\text{ZnC}_{16}\text{H}_{16}\text{O}_2\text{N}_6\text{S}_2] \cdot 2\text{H}_2\text{O}$



723

724

Figure: TGA and DTG curve of $[\text{CdC}_{18}\text{H}_{22}\text{O}_2\text{N}_6\text{S}_2]$

725